candidates, because they are usually high-risk patients with multiple comorbidities. Moreover, hilar lymph nodes cannot be assessed by mediastinoscopy. Endobronchial ultrasound-guided transbronchial needle aspiration (EBUS-TBNA) is a novel, minimally invasive modality that enables the assessment of mediastinal and hilar lymph nodes with a high sensitivity.[14–19]

In this study, we evaluated the utility of EBUS-TBNA for lymph node staging in patients with non-small cell lung cancer (NSCLC) who are potential candidates for CIRT.

PATIENTS AND METHODS

Patients

All patients referred to CIRT were initially diagnosed and staged at the referring hospital and also evaluated for operability. Patients referred to CIRT were all judged as inoperable or the patients refused surgical resection. Potential candidates for CIRT underwent a full evaluation at the Research Center Hospital for Charged Particle Therapy (NIRS). The indication for CIRT was based on histologic evidence for the peripheral type of stage I NSCLC. All patients had a performance status score between 0 and 2 according to the World Health Organization guidelines. Patients had to have no history of prior radiotherapy to the target or chemotherapy within 4 weeks before CIRT. For staging, patients were evaluated by ^{11}C-methionine-PET-CT that was routinely used for confirmation of metastases. The ^{11}C-methionine accumulation of lymph nodes was assessed semiquantitatively by analysis of the tumor-to-muscle ratio (TMR). The tumor-to-muscle ratio cutoff value for diagnosis of metastasis was determined as 4.1 following the previous results.[20] If there were abnormal accumulations in mediastinal and/or hilar lymph nodes, further investigation was required for final confirmation. From April 2005 to December 2007, 49 patients with abnormal ^{11}C-methionine-PET-CT accumulations in the mediastinum and/or hilum were evaluated by EBUS-TBNA before CIRT. Lymph node stations and numbers were determined according to the *Unio Internationalis Contra Cancrum* tumor, node, metastasis classification.[21] Patients without mediastinal and/or hilar lymph node metastases underwent CIRT; however, those with lymph node metastases underwent other types of treatment. All patients who received CIRT had routine follow-ups at the NIRS including CT scan of the chest and abdomen, ^{11}C-methionine-PET-CT, and brain MRI. EBUS-TBNA diagnosis was confirmed either by restaging by EBUS-TBNA or clinical follow-up.

This study was approved by the ethical committee of Graduate School of Medicine, Chiba University (No. 825).

Endobronchial Ultrasound-Guided Transbronchial Needle Aspiration

EBUS-TBNA was performed on an outpatient basis under conscious sedation. Local anesthesia was achieved using nebulized 1% lidocaine solution (5 mL) to the pharynx. A bolus dose of 2 mL of 1% lidocaine was used during the procedure. The bronchoscope was inserted orally with conscious sedation using midazolam. Patients were monitored by electrocardiograph, pulse oximetry, and blood pressure without the presence of an anesthesiologist.

Convex prove-EBUS (BF-UC260F-OL8, Olympus, Tokyo, Japan) was used for the examination of mediastinal and hilar lymph nodes. The convex prove-EBUS was integrated with a convex transducer (7.5 MHz) that scanned parallel to the insertion direction of the bronchoscope. Images could be obtained by directly contacting the probe or by attaching a balloon to the tip and inflating with saline. The ultrasound image was processed using a dedicated ultrasound scanner (EU-C2000, Olympus, Tokyo, Japan) and was visualized along with the conventional bronchoscopy image on the same monitor. A dedicated 22-gauge needle was used to perform transbronchial aspiration (NA-201SX-4022, Olympus, Tokyo, Japan).

After the needle is passed into the node, the internal stylet is moved in and out a short distance to clean out the internal lumen that may be plugged with bronchial wall. The internal stylet is then removed. The internal stylet was removed, and negative pressure was applied using a syringe. The needle was moved back and forth inside the tumor. Finally, the needle was retrieved, and the internal stylet was used once again to push out the histologic core.[15] Using this method, histologic cores and cytologic specimens were obtained. The aspirated material was smeared onto glass slides. Smears were air dried and immediately stained by Diff-Quik staining for immediate interpretation by an onsite cytopathologist to confirm adequate cell material. Papanicolaou and light microscopy were also done by an independent cytopathologist who was blinded to the details of the cases. The histologic cores were fixed with formalin and stained with hematoxylin and eosin. Immunohistochemistry was used for firm diagnosis. If there were adequate amount of lymphocytes without malignant cells or lymph node fragment without malignant cells, this was defined as benign lymph nodes.

Carbon Ion Radiotherapy

Carbon ion beams with 290, 350, and 400 meV/nucleon energies were generated in the Heavy Ion Medical Accelerator in Chiba. To compensate for tumor thickness, therapy was delivered by spread-out Bragg peaks.[22,23] Patients were immobilized with custom-made devices. CT planning was performed using the HIPLAN system, which was specifically developed for three-dimensional treatment planning with CT images using respiratory gating. A respiratory gating irradiation system was used to minimize respiratory motion of the tumor and to reduce the treatment volume.[24] The carbon ion radiation dose was expressed in Gray equivalents (GyE). The GyE values were calculated by multiplying the carbon physical dose (Gy) with the Relative Biologic Effectiveness factor, which was approximately 3.0.[23] The patients who received CIRT were irradiated in several protocols in the NIRS. The irradiation ranged from a total dose of 36.0 GyE with a regimen of 1 fraction to a total dose of 72.0 GyE with a regimen of 16 fractions (mean radiation dose was 49.50 GyE, 3.34 fractions). Our routine follow-up for patients post-CIRT includes clinic visits at 1, 3, 6, 9 months, thin slice CT (1–3 mm thick) every 3 months, and ^{11}C-methionine-PET-CT and brain MRI 1 and 3 months after treatment.

Data Analysis

The diagnostic accuracy rate was calculated using standard definitions.

RESULTS

Patient Characteristics

One hundred twenty-five lymph nodes (86 mediastinal and 39 hilar lymph nodes) from 49 patients with NSCLC were evaluated by EBUS-TBNA in this study. The characteristics of the 49 patients are listed in Table 1. All patients enrolled in this study showed abnormal ^{11}C-methionine-PET-CT accumulations in mediastinal and/or hilar lymph nodes. Clinical stages based on the results of ^{11}C-methionine-PET-CT were four cases of N1 disease, 42 cases of N2 disease, and three cases of N3 disease. The reasons for CIRT were as follows: 31 cases had low pulmonary functions and were determined inoperable by referring surgeons, six cases had cardiovascular disease, four cases were of advanced age with poor systemic conditions, and eight cases refused surgery for personal reasons.

Lymph Node Evaluations

All positive lymph nodes on PET-CT were assessed and all lymph nodes accessible by EBUS-TBNA; the mean number of evaluated lymph nodes was 2.55 stations per patient (range 1–5 stations per patient) (Table 2). The right lower paratracheal lymph node (no. 4R) was most often examined with 38 nodes, followed by 31 for subcarinal lymph nodes (no. 7), 29 for interlobar lymph nodes (no. 11), eight for right upper paratracheal lymph nodes (no. 2R) and eight left lower paratracheal lymph nodes (no. 4L), seven for lobar lymph nodes (no. 12), three for hilar lymph nodes (no. 10), and one for a retrotracheal lymph node (no. 3). Lymph node sizes on CT varied from 5 to 19 mm in the short axis with an average of 9.5 mm, and the sizes by endobronchial ultrasound varied from 3.1 to 22.6 mm in the short axis with an average of 9.01 mm (Table 2).

TABLE 1. Patient Characteristics

Age (yr)	
Average	75.2
Range	55–87
Sex (n = 49)	
Male	38
Histology	
Adenocarcinoma	26
Squamous cell carcinoma	19
Large cell carcinoma	1
Non-small cell lung cancer	3
PET-CT N stage	
N1 disease	4
N2 disease	42
N3 disease	3
Reason for CIRT	
Low pulmonary function	31
Cardiovascular disease	6
Other disease	4
Refused surgery	8

PET-CT, positron emission tomography-computed tomography; CIRT, carbon ion radiotherapy.

TABLE 2. Lymph Node Stations Punctured by EBUS-TBNA

	Mean (Range)	
	CT (Size/mm)	EBUS (Size/mm)
Station		
No. 2R (n = 8)	6.9 (5–12)	7.2 (5.0–10.6)
No. 3 (n = 1)	16.0	10.6
No. 4R (n = 38)	9.3 (5–19)	7.8 (3.7–22.6)
No. 4L (n = 8)	9.5 (5–15)	8.5 (4.5–12.1)
No. 7 (n = 31)	9.0 (5–15)	10.8 (3.1–19.2)
No. 10 (n = 3)	7.7 (5–12)	10.7 (9.0–12.8)
No. 11 (n = 29)	8.8 (5–15)	8.2 (4.5–12.4)
No. 12 (n = 7)	8.9 (5–12)	8.3 (5.0–14.0)
Region		
Mediastinum (n = 86)		
Hilar or Lobar (n = 39)		
Total (n = 125)	9.5 (5–19)	9.0 (3.1–22.6)

EBUS-TBNA, endobronchial ultrasound-guided transbronchial needle aspiration; CT, computed tomography.

TABLE 3. Lymph Node Sizes and Likelihood of Metastasis

	Negative for Metastasis Short Axis in mm (Range)	Positive for Metastasis Short Axis in mm (Range)
Station (metastatic rate)		
CT		
No. 4R (2/38; 5.3%)	9.4 (5–19)	7.5 (5–10)
No. 7 (4/31; 12.9%)	8.6 (5–15)	12.0 (10–15)
EBUS		
No. 4R (2/38; 5.3%)	7.8 (4.2–22.6)	6.9 (3.7–10.1)
No. 7 (4/31; 12.9%)	10.5 (3.1–19.2)	13.0 (9.2–17.7)
Average		
CT	9.0 (5–19)	10.5 (5–11)
EBUS	9.0 (3.1–22.6)	10.9 (3.7–17.7)

EBUS-TBNA, endobronchial ultrasound guided; CT, computed tomography.

EBUS-TBNA Results

We did not experience any complications related to the EBUS-TBNA procedures. Pathologic diagnosis was achieved in all patients, and lymph node metastases were diagnosed in six cases (12.2%), which included four cases of adenocarcinoma and two cases of squamous cell carcinoma. The positive cases were all N2 disease, and the metastatic sites were four cases of the subcarinal lymph node (no. 7) and two cases of the right lower paratracheal lymph node (no. 4R). In the metastatic cases, the average lymph node size in the short axis was 10.5 mm on CT (5–15 mm) and 10.9 mm on EBUS (3.7–17.7 mm) (Table 3). The cases with lymph node metastases were referred for other treatment modalities. The other 43 of 49 cases who showed no lymph node metastases by EBUS-TBNA finally received CIRT.

The results from EBUS-TBNA were confirmed either by restaging by EBUS-TBNA or by clinical follow-up (median 21.3 months, range 6–46 months). Three of 43 cases had detected interlobar lymph node metastases (no. 11) after CIRT and were judged as false-negative cases. Two of these three cases revealed metastases by EBUS-TBNA, and one case showed lymph node enlargement and multiple pulmonary metastases with abnormal accumulation on ^{11}C-methionine-PET-CT. The median period for detecting lymph node metastasis was 4.33 months after CIRT (range 4–5 months). One of the three cases had metastasis in previously aspirated lymph nodes before CIRT. The other two cases showed lymph node metastases in lymph nodes previously not evaluated by EBUS-TBNA. The diagnostic accuracy of EBUS-TBNA for diagnosis of mediastinal and hilar lymph node metastasis was 93.9% (Table 4).

DISCUSSION

Our report is the first to evaluate EBUS-TBNA for mediastinal and hilar lymph node staging in patients with NSCLC in nonoperable patients pursuing radiotherapy as a primary treatment. Lymph node staging modalities for patients who are referred for CIRT are limited, because these selected groups of individuals are likely to have multiple comorbidities and surgical interventions should be avoided. EBUS-TBNA is a novel, minimally invasive modality with a high yield for lymph node staging in lung cancer that can be performed under local anesthesia in an outpatient setting.[14–19]

The diagnostic accuracy for lymph node staging in this study was very high (93.9%), similar to previous reports on lung cancer staging.[14–19] It was also a safe procedure, even for a relatively high risk population, because we did not encounter any complications related to EBUS-TBNA. Regarding the sizes of lymph nodes, the minimum size of a positive node was 5 mm on CT and 3.7 mm on EBUS (Figure 1). Nevertheless, there were numerous negative lymph nodes >1 cm in the short axis on CT. The maximum size of a negative node was 19 mm on CT and 22.6 mm on EBUS (Figure 2). From these results, tissue confirmation should always be considered during mediastinal staging. We believe that EBUS-TBNA may also be applicable as a highly precise pretreatment staging modality for various other radical radiotherapy treatments.

Although chest CT has been used for the staging of lung cancer for a long time, its low diagnostic accuracy is a significant problem. New diagnostic modalities, such as PET and integrated PET-CT, have been reported to be useful for the detection of mediastinal and hilar lymph node metastases in patients with NSCLC.[25–27] Nevertheless, there are limitations for imaging modalities due to the lack of pathologic confirmation. Surgical candidates such as mediastinoscopy[12,13] requires general anesthesia and should be avoided in high risk patients with contraindications for surgical interventions. Furthermore, hilar lymph nodes cannot be evaluated by

TABLE 4. Comparison of EBUS-TBNA Results of Lymph Nodes with Final Diagnosis

	EBUS-TBNA Results		
Final Results	**Malignant**	**Benign**	**Total**
Malignant	6	3[a]	9
Benign	0	40	40
Total	6	43	49

[a]Two metastatic cases were detected in unevaluated lymph node.
EBUS-TBNA, endobronchial ultrasound-guided transbronchial needle aspiration.

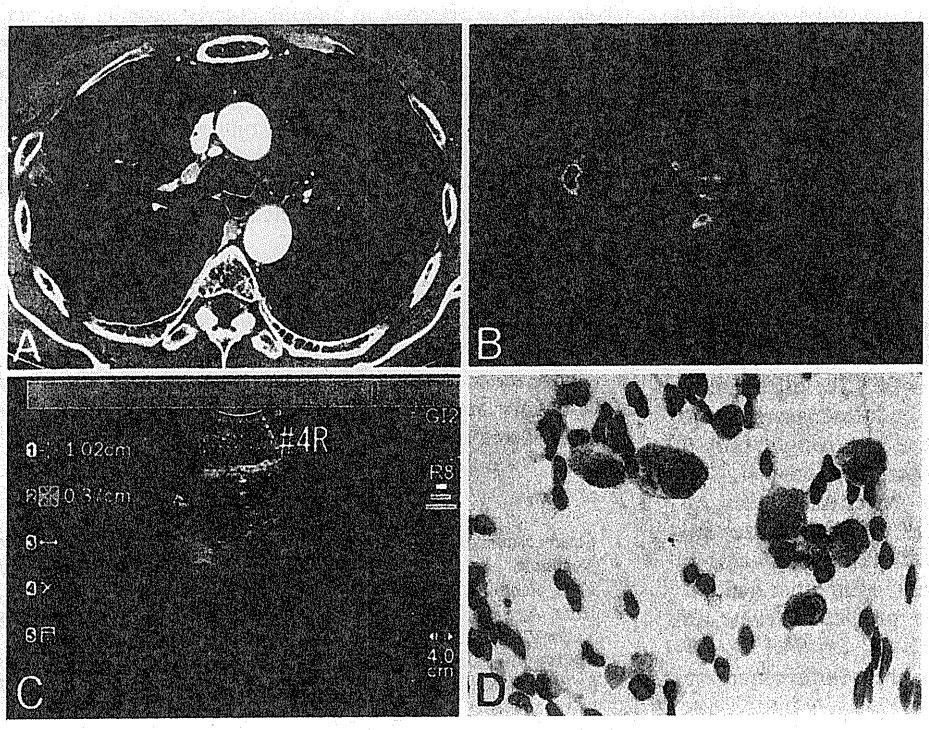

FIGURE 1. Chest computed tomography (CT), positron emission tomography (PET)-CT, endobronchial ultrasound-guided (EBUS) images, and cytology in a patient with clinical N0 non-small cell lung cancer. Although the size of the lymph node was 5 mm in the short axis (*A*), ^{11}C-methionine-PET-CT showed abnormal accumulation in the no. 4R lymph node (*B*). EBUS-TBNA from lymph node station 4R (no. 4R) with short axis of 3.7 mm (*C*) revealed adenocarcinoma (*D*) and therefore diagnosed as N2 disease.

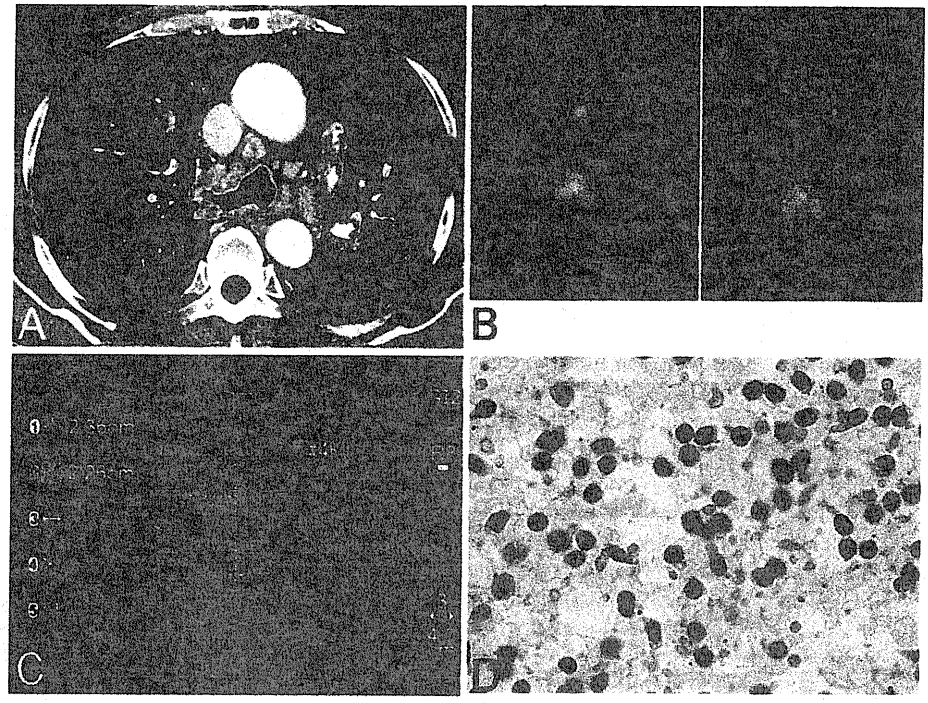

FIGURE 2. Chest computed tomography (CT), positron emission tomography (PET)-CT, endobronchial ultrasound-guided (EBUS) images, and cytology in a patient with clinical N3 non-small cell lung cancer. Significant mediastinal and hilar lymphadenopathy was observed on chest CT (*A*). FDG-PET showed abnormal accumulations in the enlarged lymph nodes (*B*). Multiple lymph node stations were aspirated by EBUS-TBNA (*C*), but results of cytology revealed only the presence of normal lymphocytes (*D*). The patient underwent carbon ion therapy.

mediastinoscopy, and N1 stations (hilar lymph nodes) should also be evaluated before CIRT.

^{11}C-methionine-PET-CT has been used for assessment of potential candidates for CIRT.[20] It is reported that ^{11}C-methionine-PET-CT could be used to evaluate the treatment effect of SRT and ^{18}F-fluorodeoxy glucose (FDG)-PET-CT.[28] In this study, abnormal accumulations in mediastinal and/or hilar lymph nodes on ^{11}C-methionine-PET-CT were evaluated. As reported previously, the negative predictive value of FDG-PET for mediastinal staging is high, and we rarely see patients with nodal disease when both CT and FDG-PET scans are negative.[16] On the other hand, false-positive results on FDG-PET scans are frequently seen in patients with lung cancer with pulmonary complications, and positive results should be carefully evaluated.[29] In our study population, 31 patients (63.3%) had similar low pulmonary function because of several pulmonary complications such as chronic obstructive pulmonary diseases. Previous reports suggest possibilities of abnormal accumulation on PET scan, which may lead to false positives in chronic inflammatory lesions.[29] Although ^{11}C-methionine-PET-CT has been shown to be more specific and sensitive compared with ^{18}F-FDG-PET for differentiating benign and malignant thoracic nodules/masses,[30] the results of our study do not support this. Surprisingly, only 9 of 49 cases (18.4%) with positive lymph nodes on ^{11}C-methionine-PET-CT were proven to have metastases by EBUS-TBNA. We can conclude that PET-positive cases are recommended for further pathologic confirmations using a proper modality such as EBUS-TBNA. On the other hand, it has been reported that the negative predictive value of PET-CT is high (^{11}C-methionine-PET-CT for 94.1%),[16,20] and it is useful to determine the indication for further invasive staging modality such as EBUS-TBNA.

CIRT is a promising modality with excellent localization and significant biologic effects on tumors. It is feasible for patients with stage I NSCLC without severe loss of respiratory functions.[31] In contrast to SRT and proton beam radiotherapy, which show good local control rate in T1 tumors, CIRT has been shown to be effective even in T2 tumors with a local control rate of more than 85%.[6–10] CIRT can be safely performed in elderly patients older than 80 years and was effective in treating elderly patients with stage I NSCLC.[5–11] The need for CIRT is increasing in an aging society, and various other irradiations have been attempted, such as proton therapy and stereotactic irradiation. Nevertheless, the success depends primarily on accurate staging before radiotherapy. Accurate lymph node staging by EBUS-TBNA will allow opportunities for high-risk inoperable patients with NSCLC to undergo minimally invasive treatment.

ACKNOWLEDGMENTS

Supported, in part, by a JSPS Fujita Memorial Fund for Medical Research Grant in 2008 for data analysis (to T.N.).

The authors thank Ms. Fumie Saegusa and Mr. Fumio Horiuchi for support with cytologic diagnosis. All authors have read and approved the final manuscript.

REFERENCES

1. Cancer Statistics in Japan Editorial Board. Cancer Statistics in Japan 08. Available at: http://ganjoho.ncc.go.jp/public/statistics/backnumber/2008_en.html. Accessed on March 22, 2009.
2. Jemal A, Siegel R, Ward E, et al. Cancer statistics, 2008. *CA Cancer J Clin* 2008;58:71–96.
3. Miyamoto T, Yamamoto N, Nishimura H, et al. Carbon ion radiotherapy for stage I non-small cell lung cancer. *Radiother Oncol* 2003;66:127–140.

4. Koto M, Miyamoto T, Yamamoto N, et al. Local control and recurrence of stage I non-small cell lung cancer after carbon ion radiotherapy. *Radiother Oncol* 2004;71:147–156.
5. Miyamoto T, Baba M, Sugane T, et al. Carbon ion radiotherapy for stage I non-small cell lung cancer using a regimen of four fractions during 1 week. *J Thorac Oncol* 2007;2:916–926.
6. Onishi H, Shirato H, Nagata Y, et al. Hypofractionated stereotactic radiotherapy (HypoFXSRT) for stage I non-small cell lung cancer: updated results of 257 patients in a Japanese multi-institutional study. *J Thorac Oncol* 2007;2:S94–S100.
7. Ball D. Stereotactic radiotherapy for nonsmall cell lung cancer. *Curr Opin Pulm Med* 2008;14:297–302.
8. Bush DA, Slater JD, Shin BB, et al. Hypofractionated proton beam radiotherapy for stage I lung cancer. *Chest* 2004;126:1198–1203.
9. Nihei K, Ogino T, Ishikura S, et al. High-dose proton beam therapy for stage I non-small-cell lung cancer. *Int J Radiat Oncol Biol Phys* 2006;65:107–111.
10. Miyamoto T, Baba M, Yamamoto N, et al. Curative treatment of Stage I non-small-cell lung cancer with carbon ion beams using a hypofractionated regimen. *Int J Radiat Oncol Biol Phys* 2007;67:750–758.
11. Sugane T, Baba M, Imai R, et al. Carbon ion radiotherapy for elderly patients 80 years and older with stage I non-small cell lung cancer. *Lung Cancer* 2009;64:45–50.
12. Hammoud ZT, Anderson RC, Meyers BF, et al. The current role of mediastinoscopy in the evaluation of thoracic disease. *J Thorac Cardiovasc Surg* 1999;118:8894–8999.
13. Luke WP, Pearson FG, Todd TR, et al. Prospective evaluation of mediastinoscopy for assessment of carcinoma of the lung. *J Thorac Cardiovasc Surg* 1986;91:53–56.
14. Yasufuku K, Chiyo M, Sekine Y, et al. Real-time endobronchial ultrasound-guided transbronchial needle aspiration of mediastinal and hilar lymph nodes. *Chest* 2004;126:122–128.
15. Yasufuku K, Chiyo M, Koh E, et al. Endobronchial ultrasound guided transbronchial needle aspiration for staging of lung cancer. *Lung Cancer* 2005;50:347–354.
16. Yasufuku K, Nakajima T, Motoori K, et al. Comparison of endobronchial ultrasound, positron emission tomography, and CT for lymph node staging of lung cancer. *Chest* 2006;130:710–718.
17. Rintoul RC, Skwarski KM, Murchison JT, et al. Endobronchial and endoscopic ultrasound-guided real-time fine-needle aspiration for mediastinal staging. *Eur Respir J* 2005;25:416–421.
18. Herth FJ, Ernst A, Eberhardt R, et al. Endobronchial ultrasound-guided transbronchial needle aspiration of lymph nodes in the radiologically normal mediastinum. *Eur Respir J* 2006;28:910–914.
19. Herth FJ, Eberhardt R, Vilmann P, et al. Real-time endobronchial ultrasound guided transbronchial needle aspiration for sampling mediastinal lymph nodes. *Thorax* 2006;61:795–798.
20. Yasukawa T, Yoshikawa K, Aoyagi H, et al. Usefulness of PET with 11C-methionine for the detection of hilar and mediastinal lymph node metastasis in lung cancer. *J Nucl Med* 2000;41:283–290.
21. Mountain CF. Revisions in the international system for staging lung cancer. *Chest* 1997;111:1710–1717.
22. Kanai T, Furusawa Y, Fukutsu K, et al. Irradiation of mixed beam and design of spread-out Bragg peak for heavy-ion radiotherapy. *Radiat Res* 1997;147:78–85.
23. Kanai T, Endo M, Minohara S, et al. Biophysical characteristics of HIMAC clinical irradiation system for heavy-ion radiation therapy. *Int J Radiat Oncol Biol Phys* 1999;44:201–210.
24. Minohara S, Kanai T, Endo M, et al. Respiratory gated irradiation system for heavy-ion radiotherapy. *Int J Radiat Oncol Biol Phys* 2000; 47:1097–1103.
25. Pozo-Rodríguez F, Martín de Nicolás JL, Sánchez-Nistal MA, et al. Accuracy of helical computed tomography and [18F] fluorodeoxyglucose positron emission tomography for identifying lymph node mediastinal metastases in potentially resectable non-small-cell lung cancer. *J Clin Oncol* 2005;23:8348–8356.
26. Gould MK, Kuschner WG, Rydzak CE, et al. Test performance of positron emission tomography and computed tomography for mediastinal staging in patients with non-small-cell lung cancer: a meta-analysis. *Ann Intern Med* 2003;139:879–892.
27. Halpern BS, Schiepers C, Weber WA, et al. Presurgical staging of non-small cell lung cancer: positron emission tomography, integrated positron emission tomography/CT, and software image fusion. *Chest* 2005;128:2289–2297.
28. Ishimori T, Saga T, Nagata Y, et al. 18F-FDG and 11C-methionine PET for evaluation of treatment response of lung cancer after stereotactic radiotherapy. *Ann Nucl Med* 2004;18:669–674.
29. Konishi J, Yamazaki K, Tsukamoto E, et al. Mediastinal lymph node staging by FDG-PET in patients with non-small cell lung cancer: analysis of false-positive FDG-PET findings. *Respiration* 2003;70:500–506.
30. Hsieh HJ, Lin SH, Lin KH, et al. The feasibility of 11C-methionine-PET in diagnosis of solitary lung nodules/masses when compared with 18F-FDG-PET. *Ann Nucl Med* 2008;22:533–538.
31. Kadono K, Homma T, Kamahara K, et al. Effect of heavy-ion radiotherapy on pulmonary function in stage I non-small cell lung cancer patients. *Chest* 2002;122:1925–1932.

ANTICANCER RESEARCH *29*: 4433-4438 (2009)

Effects of Carbon-ion Radiotherapy combined with a Novel Histone Deacetylase Inhibitor, Cyclic Hydroxamic-acid-containing Peptide 31 in Human Esophageal Squamous Cell Carcinoma

MASAYUKI KANO[1], SHIGERU YAMADA[2], ISAMU HOSHINO[1], KENTARO MURAKAMI[1], YASUNORI AKUTSU[1], HARUHITO SAKATA[1], TAKANORI NISHIMORI[1], AKIHIRO USUI[1], YUKIMASA MIYAZAWA[1], TADASHI KAMADA[2], HIROHIKO TSUJII[2] and HISAHIRO MATSUBARA[1]

[1]*Department of Frontier Surgery, Graduate School of Medicine, Chiba University, Chiba;*
[2]*National Institute of Radiological Science, Chiba, Japan*

Abstract. *Background: Carbon-ion radiotherapy has several potential advantages over X-rays. This therapy has been applied for various solid tumors including esophageal squamous cell carcinoma (SCC). However, some patients have shown resistance to this treatment. A new effective combined treatment strategy is required for improving the therapeutic effects. Histone deacetylase inhibitors (HDACIs) are new therapeutic candidates for cancer treatment. Several studies have evaluated the combination of X-rays and HDACIs, but, to date, no study has evaluated carbon-ion radiotherapy combined with HDACIs. Materials and Methods: Radio-sensitization to carbon-ion radiotherapy when combined with a novel HDACI cyclic hydroxamic-acid-containing peptide 31(CHAP31) was assessed in human esophageal SCC both in vitro and in vivo. Changes of*

Esophageal cancer is a highly malignant disease, in which progression of the disease is observed in most patients at the initial presentation (1). Neoadjuvant cytoreduction treatments are frequently used for tumor downstaging, increasing the resection rate and possibly improving survival (2). Although the combined treatment of radiation and anticancer drugs is a widely used therapeutic strategy, no satisfactory treatment regimen has yet been devised due to severe side-effects and the acquisition of resistance (3-5).

The biological effects of high linear energy transfer (LET) radiotherapy used with carbon-ion irradiation are more pronounced than low-LET conventional radiotherapy, such as X-rays or gamma rays (6). High LET radiotherapy is suitable for the local control of tumors because of its high relative biological effectiveness (RBE) and reduced oxygen

ANTICANCER RESEARCH *29*: 4433-4438 (2009)

Effects of Carbon-ion Radiotherapy combined with a Novel Histone Deacetylase Inhibitor, Cyclic Hydroxamic-acid-containing Peptide 31 in Human Esophageal Squamous Cell Carcinoma

MASAYUKI KANO[1], SHIGERU YAMADA[2], ISAMU HOSHINO[1], KENTARO MURAKAMI[1], YASUNORI AKUTSU[1], HARUHITO SAKATA[1], TAKANORI NISHIMORI[1], AKIHIRO USUI[1], YUKIMASA MIYAZAWA[1], TADASHI KAMADA[2], HIROHIKO TSUJII[2] and HISAHIRO MATSUBARA[1]

[1]*Department of Frontier Surgery, Graduate School of Medicine, Chiba University, Chiba;*
[2]*National Institute of Radiological Science, Chiba, Japan*

Abstract. *Background: Carbon-ion radiotherapy has several potential advantages over X-rays. This therapy has been applied for various solid tumors including esophageal squamous cell carcinoma (SCC). However, some patients have shown resistance to this treatment. A new effective combined treatment strategy is required for improving the therapeutic effects. Histone deacetylase inhibitors (HDACIs) are new therapeutic candidates for cancer treatment. Several studies have evaluated the combination of X-rays and HDACIs, but, to date, no study has evaluated carbon-ion radiotherapy combined with HDACIs. Materials and Methods: Radio-sensitization to carbon-ion radiotherapy when combined with a novel HDACI cyclic hydroxamic-acid-containing peptide 31(CHAP31) was assessed in human esophageal SCC both in vitro and in vivo. Changes of expression of genes related to DNA repair, by CHAP31 were assessed by quantitative real-time reverse transcriptional PCR analysis. Results: CHAP31 induced sensitization to carbon-ion radiotherapy in vitro and tumor growth was significantly suppressed by the combination of carbon-ion radiotherapy with CHAP31 in comparison to either agent alone in in vivo experiments. CHAP31 inhibited the expression of genes related to DNA repair. Conclusion: CHAP31 sensitizes SCC cells to carbon-ion radiotherapy and this combinatory treatment may be a potentially useful therapeutic strategy for esophageal SCC.*

Correspondence to: Masayuki Kano, Department of Frontier Surgery, Graduate School of Medicine, Chiba University, 1-8-1, Inohana, Chuoku, Chiba 260-0856, Japan. Tel/Fax +81 432262111, e-mail: m_kano@graduate.chiba-u.jp

Key Words: Carbon-ion radiotherapy, histone deacetylase inhibitor, esophageal cancer, squamous cell carcinoma.

Esophageal cancer is a highly malignant disease, in which progression of the disease is observed in most patients at the initial presentation (1). Neoadjuvant cytoreduction treatments are frequently used for tumor downstaging, increasing the resection rate and possibly improving survival (2). Although the combined treatment of radiation and anticancer drugs is a widely used therapeutic strategy, no satisfactory treatment regimen has yet been devised due to severe side-effects and the acquisition of resistance (3-5).

The biological effects of high linear energy transfer (LET) radiotherapy used with carbon-ion irradiation are more pronounced than low-LET conventional radiotherapy, such as X-rays or gamma rays (6). High LET radiotherapy is suitable for the local control of tumors because of its high relative biological effectiveness (RBE) and reduced oxygen enhancement ratio. Another advantage of carbon-ion radiotherapy is its superior dose distribution (7). The sharp Bragg peak of the carbon-ion enables the localization of energy to the target volume and improves the toxicity in conventional radiotherapy. However, severe late complications have been observed in patients who received high dose levels for esophageal cancer (8). Radiation pneumonitis, bone marrow suppression and other toxicities caused by carbon-ion irradiation are less frequent than those of X-ray irradiation in esophageal cancer patients. However, severe esophagitis, stenosis of the esophagus or penetration to either the trachea or aorta have been observed. Conversely, a few cases have also shown resistance to the treatment. Therefore, a suitable treatment strategy combined carbon-ion radiotherapy and other agents for cancer (9, 10) is required to resolve these problems and enhances the anti-tumor effect is needed.

The chief biological effects of radiotherapy are thought to be mediated by DNA damage, which affects cancer cell survival. The repair of DNA damage caused by carbon-ion

0250-7005/2009 $2.00+.40

irradiation is presumed to be either less or occurs more slowly than that associated with X-rays. However the existence of DNA repair of damage caused by carbon-ion irradiation has been observed in some reports (11, 12) and it could be correlated with resistance to cancer treatment. If DNA repair were to be suppressed following irradiation by charged carbon-ion particles, it could increase the anticancer effect.

Recently, histone deacetylase inhibitors (HDACIs) have been suggested as new therapeutic candidates for molecular targeted therapy for cancer (13-16). Clinical trials have demonstrated the efficacy of HDACIs for several malignant diseases (17-20). The anticancer activity by HDACIs is presumably associated with alterations in gene expression. Some authors have reported that HDACIs inhibit gene expression related to DNA repair and sensitize cells to conventional radiotherapy (21-24). Cyclic hydroxamic-acid-containing peptide 31(CHAP31) has been examined in detail for anti-cancer activity and cellular functions (25). Therefore, the current study analyzed the expression of genes related to DNA repair after CHAP31 administration and tested whether CHAP31 affects the sensitivity of human esophageal SCC cells to carbon-ion radiotherapy both *in vitro* and *in vivo*.

Materials and Methods

Cell lines and culture. The human esophageal squamous cell carcinoma (SCC) cell lines (T.Tn, TE-2) were obtained from the Japan Cell Research Bank (26, 27). A single point mutation at codon 258 (G→T: termination) in exon 7 of the p53 gene occurs on one allele of the T.Tn cells. The TE-2 line was established from a poorly differentiated human esophageal SCC containing the wild-type p53 gene. Each of these cells can form solid tumors after injection of 5×10^6 cells in the back of an athymic nude mouse. We validated the p53 genetic status by genomic sequencing (data not shown). Both the tumor cell lines were maintained as monolayer cultures in Dulbecco's modified Eagle medium (DMEM)/F-12 (DMEM: F-12=1: 1) containing 10% heat-inactivated fetal bovine serum, 0.1% L-glutamine and 0.05% penicillin-streptomycin. The media and sera were purchased from Sigma Chemical Co. (St. Louis, MO, USA).

Histone deacetylase inhibitor; cyclic hydroxamic-acid-containing peptide 31 (CHAP31). The CHAP31 was generously provided by Dr. Minoru Yoshida (Riken Advanced Science Institute, Saitama, Japan). The synthesis and purification of CHAP31 has been previously described in detail (25).

Carbon-ion beam irradiation. The cells and tumors were irradiated with carbon-ions that were accelerated ≤290 MeV/n by a HIMAC (heavy-ion medical accelerator in Chiba) synchrotron at the National Institute of Radiological Science. The irradiation system and biophysical characteristics of carbon-ion irradiation have been described elsewhere (28, 29). Briefly, the initial energy of the accelerated carbon-ion was 290 MeV/n. High-LET beams obtained by using polymethyl methacrylate absorbers with various thickness were used to change the energy of the beam (9). The LET values in all the *in vitro* and *in vivo* experiments were calculated to be 50 keV/μm. The accelerated carbon-ion irradiation, carried out at room temperature, was given 24 hr after the administration of CHAP31. The dose rate of the beam was approximately 3 Gy/min.

In vitro experiments. The cells were maintained in 25-cm^2 plastic flasks and were incubated in a 5% CO_2 incubator at 37°C. The cells were treated with CHAP31 (0, 5, 15 nM) for 0-24 h. Irradiation (0, 0.5, 1, 2, 3Gy) was carried out after CHAP31 exposure. After irradiation and/or CHAP31 exposure, the cells were removed from the culture by trypsinization in 0.05% trypsin in a 1 mM EDTA solution. The cells were plated onto 60-mm-diameter plastic dishes for the colony formation assay, using 400-30,000 cells after single treatment; 1×10^3 to 6×10^4 cells after combination treatment; 150-300 cells for the controls. The colonies were fixed and stained with a 0.2% crystal violet solution in 20% methanol after 14 days of incubation. The colonies with >50 cells were counted as survival colonies. The survival fractions were calculated as the ratio of survival colonies per number of plated cells. All the experiments were carried out in triplicate (9). Cell survival rates in comparison to the number of survival colonies without irradiation are presented.

Real-time quantitative reverse transcription-PCR (qRT-PCR). The expression changes of DNA repair related (Rad50, Mre11A, Nbs1) and cell cycle related ($p21^{WAF1}$) genes and were examined by qRT-PCR using the LightCycler technique (Roche DiagnosticsGmbH, Mannheim, Germany). Cells were seeded into a 75 cm^2 flask and incubated for 24 hours, then treated with or without an 15 nM concentration of CHAP31 before carbon-ion irradiation (2Gy) and harvested at 24 h after irradiation. Cells were washed with PBS and processed for RNA extraction with RNeasy kit (Qiagen, Inc., Chatsworth, CA). The cDNA templates for real-time PCR were synthesized from 1 μg of total RNA using SuperScript II reverse transcriptase and an oligo-dT primer. The β-actin gene served as internal control. The PCR reaction mixture consisted of DNA Master SYBR Green I mix (LightCycler-FastStart DNA Master SYBR Green I kit, Roche Diagnostics; containing Taq DNA polymerase, deoxynucleotide triphosphate, 3 mmol/L $MgCl_2$, and SYBR green dye), 0.5 μmol/L of each primer and cDNA. The PCR processes were as follows: initial denaturation at 95°C for 10 min, followed by 45 cycles of denaturation at 95°C for 15 sec, annealing at 57°C for 10 sec and elongation at 72°C for 8 to 18 sec. The Fit Points method provided by the LightCycler software was used to estimate the concentration of each sample. The expression value was calculated as follows: expression level of each mRNA/expression level of β-actin. The experiments were conducted in triplicate. The primers were chosen using Primer3 (available at http://wwwgenome.wi.mit.edu/cgi-bin/primer/primer3_www.cgi). The following primer sequences were used: Rad50, 5'-CTACCGAGTGGTGATGCTGA-3' and 5'-CCACAGTTGAGGCAGAACG-3'; Mre11A, 5'-AGTAGTGACATT TCGG-GGGGAAGG-3' and 5'-AGTAGTGACATTTCG GGAAGG-3'; Nbs1, 5'-ATGGA-GGCCATATTTCCAGAC-3' and 5'-CAAGCAGCCAGAACTTGGAAG-3'; $p21^{WAF1}$, 5'-ACTTCGACT TTGTCACCGAGA-3' and 5'-CAAGACAGTGACA GGT-CCACAT-3'; and β-actin, 5'-GAGAAAATCTGGCACCACAC-3'; and 5'-TACCCCT-CGTAGATGGGCAC-3'.

Evaluation of the effects on tumor growth. Balb/c nu/nu athymic male mice (6-8 weeks old; CLEA Japan, Inc. Tokyo, Japan) were used. The animal experiments were performed at the Laboratory Animal Center of the National Institute of Radiological Science. The guidelines from the National Institute of Radiological Sciences Safety and Health Regulations for Handling Experimental Animals

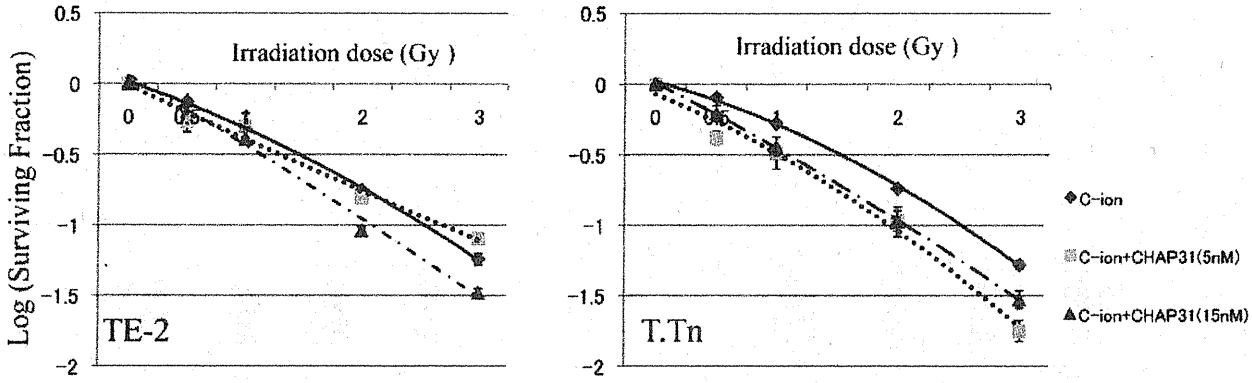

Figure 1. *In vitro growth suppression of human esophageal squamous cell carcinoma (TE-2, T.Tn) cells irradiated with carbon-ion beam with or without 24h CHAP31 exposure before irradiation. Curves are normalized to CHAP31 treatment alone. C-ion; Carbon-ion irradiation.*

(2001) were followed. The mice with 5×10^6 T.Tn or TE-2 cells were inoculated subcutaneously in 0.2 ml culture medium and randomly divided on day 0 of treatment into 4 groups as follows: i) control group; ii) CHAP31 only injection group; iii) carbon-ion irradiation only group and iv) CHAP31 injection before and after carbon-ion irradiation group to adjust mean tumor volume of each group. CHAP31 was administered to the tumor-bearing mice by intravenous (*i.v.*) injections with a 27-gauge hypodermic needle at a dose of 5 mg/kg on day 1, 4, and 7. On day 2, 24 h after the first CHAP31 injection, the tumor was irradiated with a single dose of 3 Gy. The mice were anesthetized by intraperitoneal injections of pentabarbiturate prior to irradiation. The tumor size was measured with calipers every 5 days over a period of 35 days. The tumor volume was calculated according to the (length × width^2)/2 and presented as the mean (± standard deviation (SD)) mm^3.

Results

In vitro cytotoxic effects of CHAP31 and carbon-ion irradiation. The *in vitro* survival curves of the T.Tn and TE-2 cells treated for 24 h with CHAP31 before carbon-ion irradiation of are shown in Figure 1. The combined therapy was stronger than either single therapy used alone in regard to its anticancer efficacy. In addition, the relationship between CHAP31 administration and carbon-ion irradiation was statistically significant analyzed using two-way ANOVA for each cell line ($p<0.001$).

Effect of CHAP31 on expression of genes related to DNA repair and cell cycle. The gene expression levels of Rad50, Mre11A and Nbs1 decreased after 24 h CHAP31 administration (Figure 2a, 2b). The gene expression levels of p21^{WAF1} increased. The gene expression of Rad50 and Mre11A in the TE-2 cells of Mre11A in the T.Tn cells was increased after carbon-ion irradiation. CHAP31 inhibited the gene expressions increased by carbon-ion irradiation (Figure 2c, 2d).

In vivo effects of carbon-ion irradiation and CHAP31 administration. The growth suppression effects evaluated by the tumor volumes are shown in Figure 3. At day 35, the mean tumor volume of the combined treatment group was significantly smaller than the tumor volume in either single therapy group ($p<0.05$, Mann-Whitney *U*-test, respectively).

Discussion

The mechanism by which HDACIs sensitize cells to conventional radiotherapy is thought to be due to cell cycle G2/M arrest, inhibition of DNA repair and increases in DNA double strand breaks. HDACIs are thought to alter gene expression by the hyperacetylation of histone tails.

Recent studies also reported that HDACIs exert cell cycle arrest by inducing p21^{WAF1} in some other cell lines (16, 30-32).

The Mre11-Rad50-Nbs1 (MRN) complex, consisting of proteins encoded by the genes Mre11, Rad50 and Nbs1, plays a crucial role in DNA double-strand break (DSB) repair (33) (Figure 4). The complex has many biological functions, including the formation of double strand breaks during meiosis, homologous recombination, telomere maintenance, S-phase checkpoint and genome stability during replication. The current results showed that CHAP31 suppressed the expression of this complex. This suggests that HDACs could inhibit the function of the MRN complex.

In the present study, the administration of CHAP31 and carbon-ion beam irradiation efficiently enhanced the anti-tumor effect on human esophageal SCC in both *in vitro* and *in vivo* experiments. The *in vitro* experiments showed a significant synergistic effect as suggested by the two-way ANOVA of each cell line, between carbon-ion irradiation and CHAP31 administration for esophageal SCC. CHAP31 sensitized the esophageal SCC cells *in vitro* (data not shown).

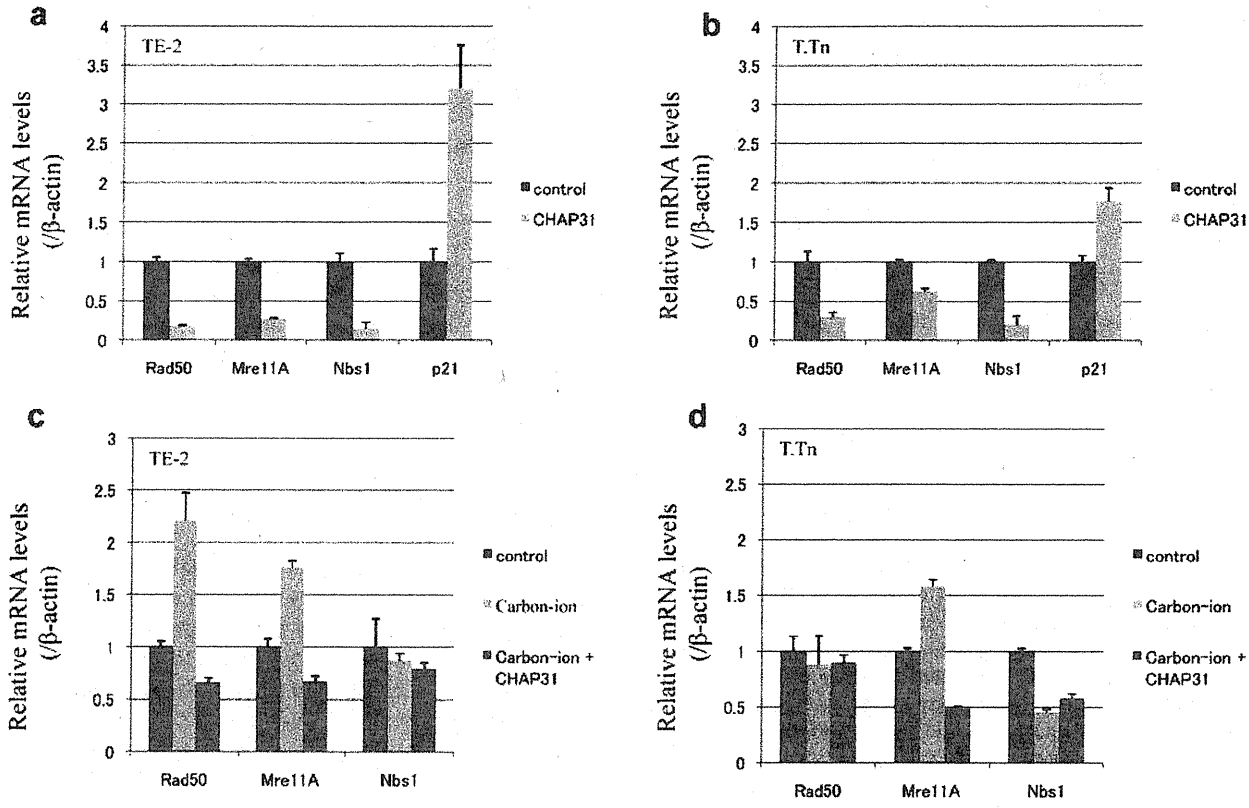

Figure 2. *The changes of gene expression of Rad50, Mre11A, Nbs1 and p21^{WAF1} after CHAP31 administration by quantitative real-time reverse transcription-PCR (qRT-PCR) analysis. Values shown are means ±standard deviation of 3 independent experiments. Control: untreated cells.*

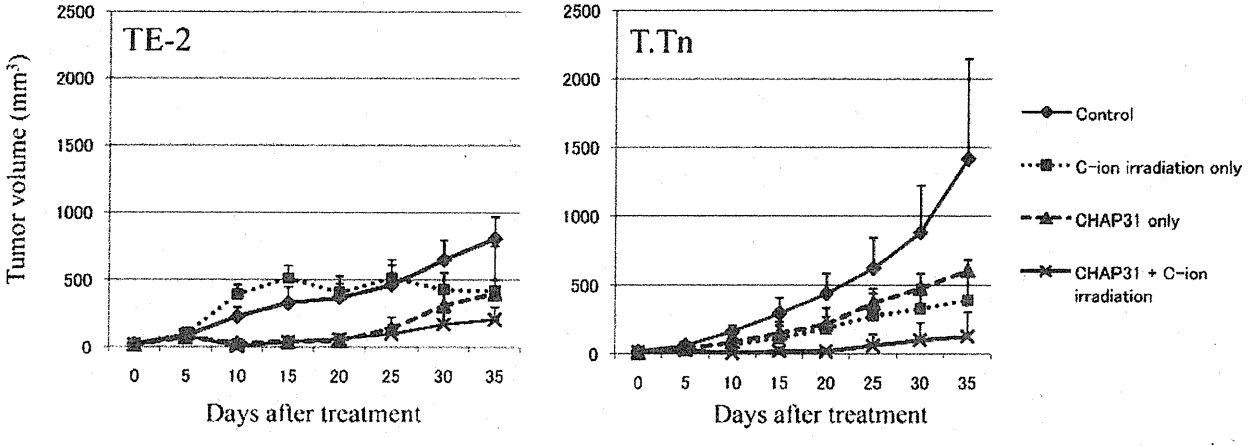

Figure 3. *The effect of carbon-ion 3 Gy irradiation and/or CHAP31 (5mg/kg i.v.) on in vivo tumor growth of esophageal squamous cell carcinoma (TE-2, T.Tn). Values represent the mean and standard deviation of 5 mice. Control: untreated.*

In the *in vivo* experiments, CHAP31 was administered to mice by *i.v.* injections. This method was considered an appropriate preclinical model. The combination therapy showed a statistically significant growth suppression in comparison to each of the single treatment groups. However, there was no significant effect of the combination of CHAP31 administration and carbon-ion irradiation based on two-way ANOVA. The *in vivo* tumor growth might be affected by

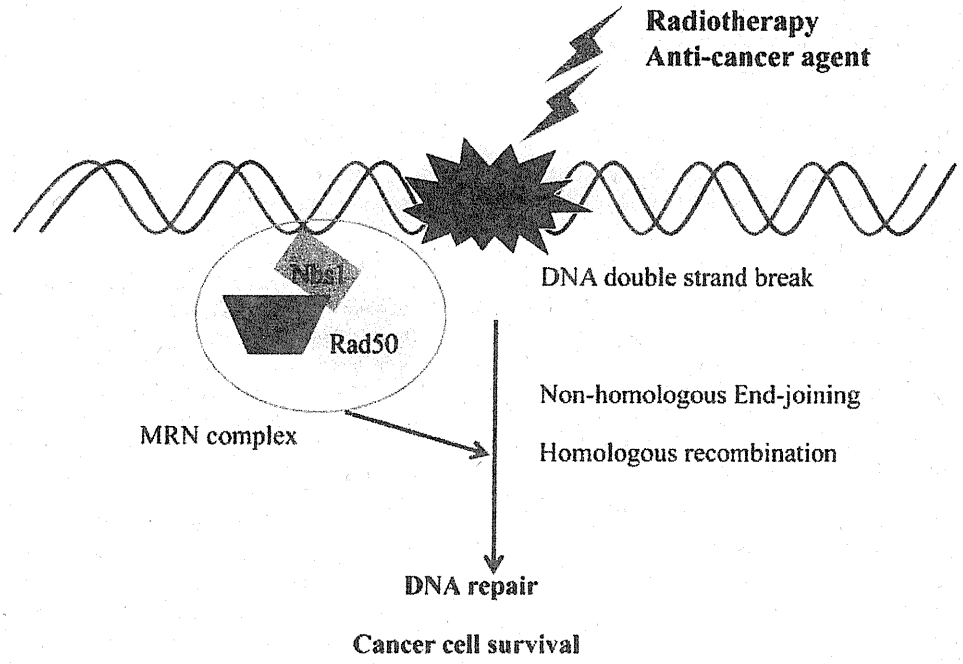

Figure 4. *The Mre11-Rad50-Nbs1 (MRN) complex plays a crucial role in DNA double-strand break repair.*

other elements such as the tumor stroma, paracrine factors, tumor vessels, or drug delivery and so on. Carbon-ion radiotherapy itself is an effective therapeutic modality for esophageal SCC. In this study, CHAP31 treatment was therefore shown to enhance the antitumor effects of carbon-ion irradiation on a human esophageal SCC cell line. Molecular targeted drugs such as HDACIs have demonstrated low toxicity and some agents are already used clinically. The use in combination with a carbon-ion localized radiation field may therefore be a less toxic and more effective therapeutic combination modality for esophageal cancer.

Acknowledgements

This work was supported in part by the Global COE Program (Global Center for Education and Research in Immune System Regulation and Treatment), Ministry of Education, Culture, Sports, Science and Technology (MEXT), Japan.

References

1 Isono K and Ochiai T: Recent advances of treatment of cancer of the esophagus. Ann Cancer Res Ther *1*: 9-16, 1992.
2 Ancona E, Ruol A, Castoro C, Chiarion-Sileni V, Merigliano S, Santi S, Bonavina L and Peracchia A: First-line chemotherapy improves the resection rate and long-term survival of locally advanced (T4, any N, M0) squamous cell carcinoma of the thoracic esophagus: Final report on 163 consecutive patients with 5-year follow-up. Ann Surg *226*: 714-723, 1997.
3 Houghton JA, Weiss KD, Williams LG, Torrance PM and Houghton PJ: Relationship between 5-fluoro-2'-deoxyuridylate, 2'-deoxyuridylate, and thymidylate synthase activity subsequent to 5-fluorouracil administration, in xenografts of human colon adenocarcinomas. Biochem Pharmacol *35*: 1351-1358, 1986.
4 Shimada H, Hoshino T, Okazumi S, Matsubara H, Funami Y, Nabeya Y, Hayashi H, Takeda A, Shiratori T, Uno T, Ito H and Ochiai T: Expression of angiogenic factors predicts response to chemoradiotherapy and prognosis of oesophageal squamous cell carcinoma. Br J Cancer *86*: 552-557, 2002.
5 Aschele C, Sobrero A, Faderan MA and Bertino JR: Novel mechanisms of resistance to 5-fluorouracil in human colon cancer (HCT-8) subline following exposure to two different clinically relevant dose schedules. Cancer Res *52*: 1855-1864, 1992.
6 Ritter MA, Cleaver JE and Tobias C: High-LET radiations induce a large proportion of non-rejoining DNA breaks. Nature *266*: 653-655, 1977.
7 Chen GT, Castro JR and Quivey JM: Heavy charged particle radiotherapy. Ann Rev Biophys Bioeng *10*: 499-529, 1981.
8 Tsujii H, Mizoe JE, Kamada T, Baba M, Kato S, Kato H, Tsuji H, Yamada S, Yasuda S, Ohno T, Yanagi T, Hasegawa A, Sugawara T, Ezawa H, Kandatsu S, Yoshikawa K, Kishimoto R and Miyamoto T: Overview of clinical experiences on carbon ion radiotherapy at NIRS. Radiother Oncol *73(Suppl 2)*: S41-49, 2004.
9 Oohira G, Yamada S, Ochiai T, Matsubara H, Okazumi S, Ando K, Tsujii H, Hiwasa T and Shimada H: Growth suppression of esophageal squamous cell carcinoma induced by heavy carbon-ion beams combined with p53 gene transfer. Int J Oncol *25*: 563-569, 2004.

10 Kitabayashi H, Shimada H, Yamada S, Yasuda S, Kamata T, Ando K, Tsujii H and Ochiai T: Synergistic growth suppression induced in esophageal squamous cell carcinoma cells by combined treatment with docetaxel and heavy carbon-ion beam irradiation. Oncol Rep *15(4)*: 913-918, 2006.

11 Hirayama R, Furusawa Y, Fukawa T and Ando K: Repair kinetics of DNA-DSB induced by X-rays or carbon ions under oxic and hypoxic conditions. J Radiat Res (Tokyo) *46(3)*: 325-332, 2005.

12 Yashiro T, Koyama-Saegusa K, Imai T, Fujisawa T and Miyamoto T: Inhibition of potential lethal damage repair and related gene expression after carbon-ion beam irradiation to human lung cancer grown in nude mice. J Radiat Res (Tokyo) *48(5)*: 377-383, 2007.

13 Walkinshaw DR and Yang XJ: Histone deacetylase inhibitors as novel anticancer therapeutics. Curr Oncol *15(5)*: 237-243, 2008.

14 Lee EJ, Lee BB, Kim SJ, Park YD, Park J and Kim DH: Histone deacetylase inhibitor scriptaid induces cell cycle arrest and epigenetic change in colon cancer cells. Int J Oncol *33(4)*: 767-776, 2008.

15 Law AY, Lai KP, Lui WC, Wan HT and Wong CK: Histone deacetylase inhibitor-induced cellular apoptosis involves stanniocalcin-1 activation. *314(16)*: 2975-2984, 2008.

16 Hoshino I, Matsubara H, Hanari N, Mori M, Nishimori T, Yoneyama Y, Akutsu Y, Sakata H, Matsushita K, Seki N and Ochiai T: Histone deacetylase inhibitor FK228 activates tumor suppressor Prdx1 with apoptosis induction in esophageal cancer cells. Clin Cancer Res *11(21)*: 7945-7952, 2005.

17 Whitehead RP, Rankin C, Hoff PM, Gold PJ, Billingsley KG, Chapman RA, Wong L, Ward JH, Abbruzzese JL and Blanke CD: Phase II trial of romidepsin (NSC-630176) in previously treated colorectal cancer patients with advanced disease: a Southwest Oncology Group study (S0336). Invest New Drugs [Epub ahead of print], 2008.

18 de Bono JS, Kristeleit R, Tolcher A, Fong P, Pacey S, Karavasilis V, Mita M, Shaw H, Workman P, Kaye S, Rowinsky EK, Aherne W, Atadja P, Scott JW and Patnaik A: Phase I pharmacokinetic and pharmacodynamic study of LAQ824, a hydroxamate histone deacetylase inhibitor with a heat shock protein-90 inhibitory profile, in patients with advanced solid tumors. Clin Cancer Res *14(20)*: 6663-6673, 2008.

19 Braiteh F, Soriano AO, Garcia-Manero G, Hong D, Johnson MM, Silva Lde P, Yang H, Alexander S, Wolff J and Kurzrock R: Phase I study of epigenetic modulation with 5-azacytidine and valproic acid in patients with advanced cancers. Clin Cancer Res *14(19)*: 6296-6301, 2008.

20 Sharma S, Symanowski J, Wong B, Dino P, Manno P and Vogelzang N: A Phase II Clinical Trial of Oral Valproic Acid in Patients with Castration-Resistant Prostate Cancers Using an Intensive Biomarker Sampling Strategy. Transl Oncol *1(3)*: 141-147, 2008.

21 Chinnaiyan P, Cerna D, Burgan WE, Beam K, Williams ES, Camphausen K and Tofilon PJ: Postradiation sensitization of the histone deacetylase inhibitor valproic acid. Clin Cancer Res *14(17)*: 5410-5415, 2008.

22 Harikrishnan KN, Karagiannis TC, Chow MZ and El-Osta A: Effect of valproic acid on radiation-induced DNA damage in euchromatic and heterochromatic compartments. Cell Cycle *7(4)*: 468-476, 2008.

23 Cuneo KC, Fu A, Osusky K, Huamani J, Hallahan DE and Geng L: Histone deacetylase inhibitor NVP-LAQ824 sensitizes human nonsmall cell lung cancer to the cytotoxic effects of ionizing radiation. Anticancer Drugs *18(7)*: 793-800, 2007.

24 Entin-Meer M, Yang X, VandenBerg SR, Lamborn KR, Nudelman A, Rephaeli A and Haas-Kogan DA: *In vivo* efficacy of a novel histone deacetylase inhibitor in combination with radiation for the treatment of gliomas. Neuro Oncol *9(2)*: 82-88, 2007

25 Komatsu Y, Tomizaki K, Tsukamoto M, Kato T, Nishino N, Sato S, Yamori T, Tsuruo T, Furumai R, Yoshida M, Horinouchi S and Hayashi H: Cyclic Hydroxamic-acid-containing Peptide 31, a Potent Synthetic Histone Deacetylase Inhibitor with Antitumor Activity. Cancer Res *61*: 4459-4466, 2001.

26 Takahashi K, Kanazawa H, Chan H, Hosono T, Takahara M and Sato K: A case of esophageal carcinoma metastatic to the mandible and characterization of two cell lines (T.T. and T.Tn) Jpn. J Oral Maxillofac Surg *36*: 307-316, 1990.

27 Nishihira T, Kasai M, Mori S, Watanabe T, Kuriya Y, Suda M, Kitamura M, Hirayama K, Akaishi T and Sasaki T: Characteristics of two cell lines (TE-1 and TE-2) derived from human squamous cell carcinoma of the esophagus. Gann *70*: 575-584, 1979.

28 Kanai T, Endo M, Minohara S, Miyahara N, Koyama-ito H, Tomura H, Matsufuji N, Futami Y, Fukumura A, Hiraoka T, Furusawa Y, Ando K, Suzuki M, Soga F and Kawachi K: Biophysical characteristics of HIMAC clinical irradiation system for heavy-ion radiation therapy. Int J Radiat Oncol Biol Phys *44*: 201-210, 1999.

29 Ando K, Koike S, Nojima K, Chen YJ, Ohira C, Ando S, Kobayashi N, Ohbuchi T, Shimizu W and Kanai T: Mouse skin reactions following fractionated irradiation with carbon ions. Int J Radiat Biol *74*: 129-138, 1998.

30 Huang L and Pardee AB: Suberoylanilide hydroxamic acid as a potential therapeutic agent for human breast cancer treatment. Mol Med *6*: 849-866, 2000.

31 Sasakawa Y, Naoe Y, Inoue T, Sasakawa T, Matsuo M, Manda T and Mutoh S: Effects of FK228, a novel histone deacetylase inhibitor, on human lymphoma U-937 cells *in vitro* and *in vivo*. Biochem Pharmacol *64*: 1079-1790, 2002.

32 Sowa Y, Orita T, Minamikawa S, Nakano K, Mizuno T, Nomura H and Sakai T: Histone deacetylase inhibitor activates the WAF1/Cip1 gene promoter through the Sp1sites. Biochem Biophys Res Commun *241*: 142-150, 1997.

33 Bartkova J, Tommiska J, Oplustilova L, Aaltonen K, Tamminen A, Heikkinen T, Mistrik M, Aittomäki K, Blomqvist C, Heikkilä P, Lukas J, Nevanlinna H and Bartek J: Aberrations of the MRE11-RAD50-NBS1 DNA damage sensor complex in human breast cancer: MRE11 as a candidate familial cancer-predisposing gene. Mol Oncol *2(4)*: 296-316, 2008.

Received May 25, 2009
Revised August 14, 2009
Accepted September 1, 2009

ELSEVIER

Int. J. Radiation Oncology Biol. Phys., Vol. 74, No. 1, pp. 15–20, 2009

0360-3016/09/$–see front matter

doi:10.1016/j.ijrobp.2008.07.056

CLINICAL INVESTIGATION **Head and Neck**

MUCOSAL MALIGNANT MELANOMA OF THE HEAD AND NECK TREATED BY CARBON ION RADIOTHERAPY

TAKESHI YANAGI, M.D., PH.D.,* JUN-ETSU MIZOE, M.D., PH.D.,* AZUSA HASEGAWA, D.D.S., PH.D.,* RYO TAKAGI, D.D.S., PH.D.,* HIROKI BESSHO, D.D.S., PH.D.,* TAKESHI ONDA, D.D.S., PH.D.,* TADASHI KAMADA, M.D., PH.D.,* YOSHITAKA OKAMOTO, M.D., PH.D.,† AND HIROHIKO TSUJII, M.D., PH.D.*

*National Institute of Radiological Sciences, Research Center Hospital for Charged Particle Therapy, Chiba, Japan; and †Division of Otorhinolaryngology, Graduate School of Medicine and School of Medicine, Chiba University, Chiba, Japan

Purpose: To evaluate the efficacy of carbon ion radiotherapy for mucosal malignant melanoma of the head and neck.

Methods and Materials: Between 1994 and 2004, 72 patients with mucosal malignant melanoma of the head and neck were treated with carbon ion beams in three prospective studies. Total dose ranged from 52.8 GyE to 64 GyE given in 16 fixed fractions over 4 weeks. Clinical parameters including gender, age, Karnofsky index, tumor site, tumor volume, tumor status, total dose, fraction size, and treatment time were evaluated in relation to local control and overall survival.

Results: The median follow-up period was 49.2 months (range, 16.8–108.5 months). Treatment toxicity was within acceptable limits, and no patients showed Grade 3 or higher toxicity in the late phase. The 5-year local control rate was 84.1%. In relation to local control, there were no significant differences in any parameters evaluated. The 5-year overall and cause-specific survival rates were 27.0% and 39.6%, respectively. For overall survival, however, tumor volume (≥100 mL) was found to be the most significant prognostic parameter. Of the patients who developed distant metastasis, 85% were free from local recurrence.

Conclusion: Carbon ion radiotherapy is a safe and effective treatment for mucosal malignant melanoma of the head and neck in terms of high local control and acceptable toxicities. Overall survival rate was better than in those treated with conventional radiotherapy and was comparable to that with surgery.

Carbon ion radiotherapy, Mucosal malignant melanoma, Heavy ion beam, Linear energy transfer (LET), Head and neck.

INTRODUCTION

The worldwide incidence of malignant melanoma seems to be influenced by racial and/or geographical differences. For example, the rates are 16.2 per 100,000 in the United States and 0.383 per 100,000 in Japan (1–3). However, the incidence of malignant melanoma arising from mucosal membrane is relatively high in Japan compared with Western countries. Regarding the head-and-neck region, it constitutes approximately 30% of all malignant melanomas in Japan, whereas it represents only 1% in Western countries (4, 5). Thus, the rate of patients with mucosal malignant melanoma of the head and neck in both Japan and the United States comes to approximately 0.1 per 100,000, suggesting that this specific condition may generally be rare worldwide (6).

Because of this low incidence, the number of patients with mucosal malignant melanoma of the head and neck encountered by a single facility is also small, and it has as yet not been possible to establish an optimum treatment modality. Surgical resection has traditionally been the primary mode of treatment for this disease. Wide en-bloc excision is needed for the complete removal of the tumor, but in the case of a large tumor mass or involvement of adjacent critical structures, surgery is counter-indicated for cosmetic and functional reasons. Furthermore, even when total resection of the gross tumor has been performed, the outcome in terms of local tumor control and long-term survival has not been satisfactory. It is reported that the local recurrence rate is approximately 50%, and the overall postsurgery 5-year survival rate is 28–36% (7–13).

Malignant melanoma has long been regarded as radioresistant because it often demonstrated poor regression after photon radiotherapy, with recurrence developing within

Reprint requests to: Takeshi Yanagi, M.D., Ph.D., Department of Radiation Medicine, Research Center of Charged Particle, National Institute of Radiological Sciences, Anagawa 4-9-1, Inage-ku, Chiba City, Chiba Prefecture 263-8555, Japan. Tel: (+81) 43-206-3306; Fax: (+81) 43-256-6506; E-mail: t_yanagi@nirs.go.jp

Conflict of interest: none.

Received March 31, 2008, and in revised form July 10, 2008. Accepted for publication July 24, 2008.

1 year (14, 15). It is reported, however, that the use of a high dose per fraction might improve the local response, with the 3-year local control rate being 30–60% (16, 17). This suggests that irradiation could be a definitive treatment modality for cure if administered appropriately.

In 1994, carbon ion radiotherapy was initiated at the National Institute of Radiological Sciences (NIRS) in Japan (18–20). Carbon ion beams provide superior physical dose distribution because of their finite range in the target tissue, and they possess a biological advantage due to their high relative biological effectiveness (RBE) in the Bragg peak (21, 22). It is therefore reasonable to assume that carbon ion beams might be superior to X-rays for the management of tumors characterized by poor radiosensitivity, such as malignant melanoma.

This report presents the results of a radiotherapy regimen for 72 patients with mucosal malignant melanoma of the head and neck treated with carbon ion beams at NIRS.

METHODS AND MATERIALS

Patients

From June 1994 through February 2004, a total of 156 patients with mucosal malignant melanoma were treated with carbon ion beams in three prospective trials: a Phase I/II study using an 18-fraction schedule ($n = 2$), a Phase I/II study using a 16-fraction schedule ($n = 9$), and a Phase II study ($n = 145$) with a 16-fraction schedule. The treatment techniques of the three protocols were the same except for the fractionation. The eligibility criteria were also the same. Of these patients, 72 treated with carbon ion radiotherapy on a 16-fraction schedule as primary treatment for the tumor were analyzed. Patient characteristics are shown in Table 1. All patients had gross tumors. Twenty-two patients had tumors with no previous treatment, and the remaining 50 patients had recurrent tumors after surgery or after chemotherapy. Diagnosis was histologically confirmed in all patients, and informed consent was obtained.

Table 1. Patient characteristics

Gender (M/F)	35/37
Age (y), range (median)	38–83 (64)
Karnofsky index	
60	1 (1.4)
70	7 (9.7)
80	23 (32.0)
90	41 (56.9)
Tumor site	
Nasal cavity	44 (61.1)
Ethmoid sinus	9 (12.5)
Maxillary sinus	6 (8.3)
Sphenoid sinus	1 (1.4)
Oral cavity	7 (9.7)
Pharynx	5 (7.0)
Tumor volume (ml)	
<100	35 (48.6)
≥100, <200	25 (34.7)
≥200	12 (16.7)
Tumor status	
No previous treatment	22 (16.7)
Recurrence after surgery/CT	50 (83.3)

Abbreviations: M = male; F = female; CT = chemotherapy.
Values are number (percentage) unless otherwise noted.

Carbon ion radiotherapy

The patient was positioned in a customized cradle, with the face immobilized with a low-temperature thermoplastic device. If the patient had metal prostheses that would be included in the radiation field, the prostheses were removed to avoid artifacts in the planning CT images.

A set of 2.5-mm-thick CT scans was taken for treatment planning, with the patient lying on an immobilization device. Three-dimensional treatment planning was performed using HIPLAN, a program developed at NIRS (23). This system permits the fusion of MRI images with CT images for precise delineation of the target volume. To create a clinical target volume, a margin of 5–10 mm was added to include both gross and potentially microscopic disease. Furthermore, a margin of 3–5 mm was added as an internal and setup margin around the clinical target volume to create a final planning target volume. When the tumor was located close to critical organs, such as the brain stem and spinal cord, those margins were reduced as necessary.

Dose was expressed in gray equivalent (GyE), which was calculated by multiplying the physical dose by the RBE. The clinical RBE of the carbon beam at our institute was determined according to the RBE for acute skin reaction, which was assessed to be 3.0 at the distal part of the spread-out Bragg peak (24).

At every treatment session, the patient's position was verified with a computer-aided on-line positioning system. The patient was positioned on the treatment couch with immobilization devices, and digital orthogonal X-ray images were taken and transferred to the positioning computer. The positioning images were compared with reference images that were digitally reconstructed from CT scans. If the difference in positioning was >1 mm, the treatment couch was moved until an acceptable position was attained.

Carbon ion radiotherapy was given in 16 fractions over 4 weeks, at 4 treatment days per week. The overall treatment time was 23–38 days (median, 28 days).

After radiotherapy, acute toxicity of skin, mucosa, and brain was scored according to the Radiation Therapy Oncology Group acute radiation morbidity scoring criteria, and late toxicity was scored according to the Radiation Therapy Oncology Group/European Organization for Research and Treatment of Cancer late radiation morbidity scoring scheme (25).

Local control and survival

Rates of local control, overall survival, and cause-specific survival were calculated using the Kaplan-Meier algorithm, and the potential prognostic factors (gender, age, Karnofsky index, tumor site, tumor volume, tumor status, total dose, fraction size, and treatment time) for local control and overall survival were evaluated using the log–rank test. Multivariate analysis was performed using the Cox proportional hazards model.

RESULTS

Treatment and tumor control

The median follow-up period was 49.2 months (range, 16.8–108.5 months). The cumulative 5-year local control rate for all 72 patients was 84.1% (Fig. 1). Tumor recurrence at the primary site was observed in 9 patients (12.5%) at 4.3–20.0 months (median, 13.9 months) after carbon ion radiotherapy, with 5 of the 9 subsequently receiving salvage

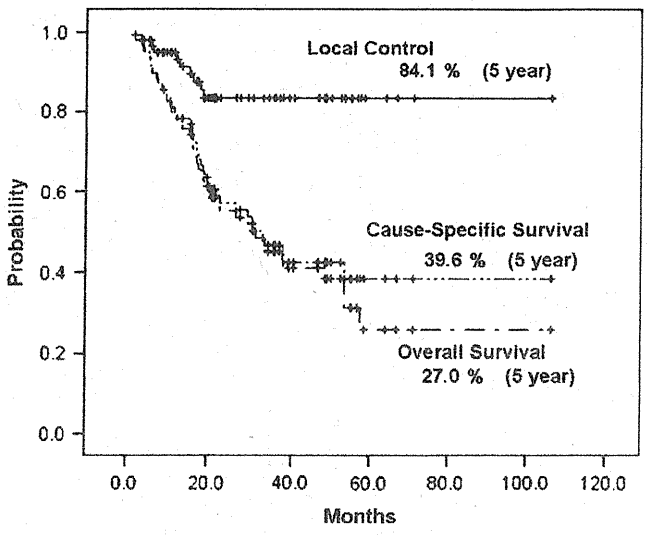

Fig. 1. Cumulative local control curve (solid line), overall survival curve, and cause-specific survival curve (broken lines) for all patients (n = 72). Five-year rates of local control, overall survival, and cause-specific survival for all patients were 84.1%, 27.0%, and 39.6%, respectively.

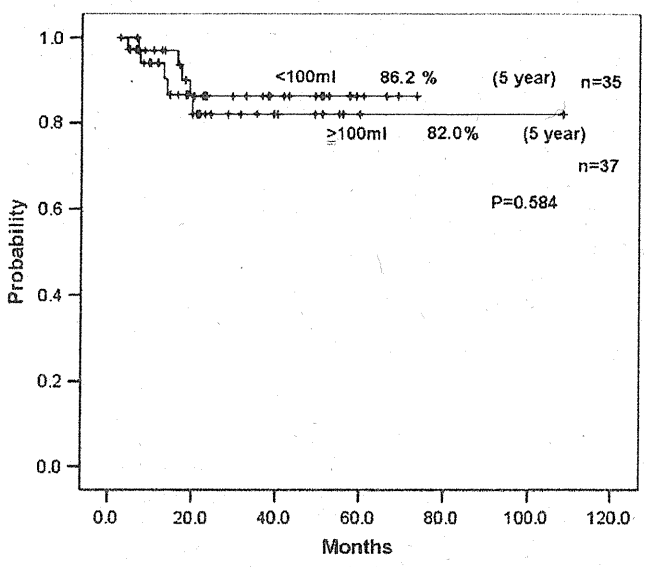

Fig. 2. Cumulative local control curves for the tumor volume subgroups (<100 mL, ≥100 ml). The 5-year local control rate for the <100 mL subgroup was 86.2%, and that for the ≥100 mL subgroup was 82.0%. There was no statistically significant difference between the two subgroups.

resection and/or chemotherapy. Three of them became disease-free. The ultimate cumulative local control rate was 88.7% at 5 years.

None of the factors evaluated by univariate analysis were correlated with local control (Table 2). Local control curves of tumor volume subgroups (<100 mL, ≥100 mL) are shown in Fig. 2, representing 86.2% and 82.0%, respectively. No statistically significant differences were found between the two groups.

Neck lymph node metastasis was observed in 13 patients (18.1%), and 5 of these 13 patients had no local recurrence at the primary site. The duration until lymph node metastasis ranged from 1.5 to 32.5 months (median, 10.1 months) after radiotherapy. Among these 13 patients, 6 underwent neck dissection followed by photon irradiation with or without chemotherapy, and their neck disease was controlled during the observation period. However, all patients with lymph node recurrence in the neck died of distant metastases within 3 years after the carbon ion treatment.

Of the total patients, 40 (55.6%) developed distant metastasis, and 34 of these 40 patients (85.0%) remained without local recurrence. Distant metastasis occurred within a period ranging from 1.1 to 60.9 months (median, 26.7 months).

Survival

The overall survival rates at 3 and 5 years were 46.1% and 27.0%, respectively, and the corresponding cause-specific survival rates were 47.7% and 39.6%, respectively (Fig. 1).

Univariate analysis on overall survival showed that tumor volume and Karnofsky index were significant factors. By multivariate analysis, only the tumor volume remained statistically significant (p = 0.001) (Table 2). The overall survival curves by tumor volume subgroup are shown in Fig. 3. Patients with smaller tumors (<100 mL) had better survival

Table 2. Univariate and multivariate analysis (n = 72)

Variable	Subgroup (n)	Local control (univariate p)	Overall survival	
			Univariate p	Multivariate p
Gender	M (35)/F (37)	0.835	0.535	—
Age (y)	<60 (24)/≥60 (48)	0.544	0.865	—
Karnofsky index	<90 (31)/≥90 (41)	0.695	0.025*	0.074
Site	Sinonasal (60)/others (12)	0.180	0.377	—
Tumor volume (ml)	<100 (35)/≥100 (37)	0.584	<0.001*	0.001*
Tumor status	No previous treatment (22)/ recurrence (50)	0.650	0.062	—
Total dose (GyE)	<57.6 (4)/≥57.6 (68)	0.364	0.607	—
Fraction size (GyE)	<3.6 (4)/≥3.6 (68)	0.364	0.607	—
Treatment time (d)	<28 (32)/≥28 (40)	0.950	0.664	—

Abbreviations as in Table 1.
* Significantly correlated.

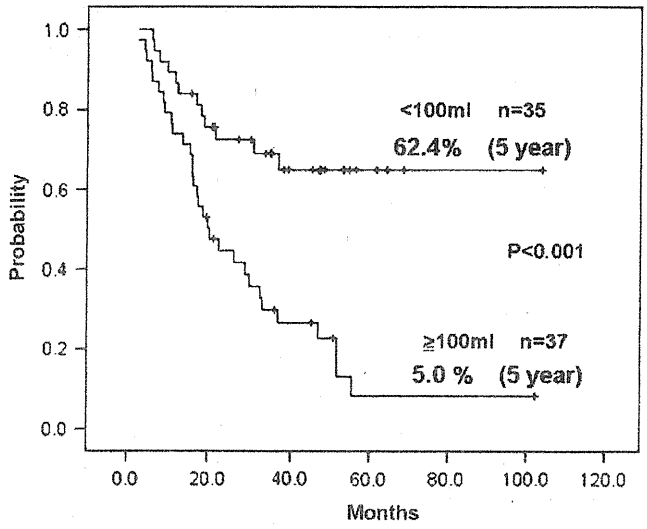

Fig. 3. Cumulative overall survival curves for the tumor volume subgroups (<100 mL, ≥100 mL). The 5-year overall survival rate for the <100 mL subgroup was 62.4%, and that for the ≥100 mL subgroup was 5.0%. A statistically significant difference was demonstrated between the two subgroups.

than those with larger tumors (≥100 mL), with statistical significance ($p < 0.001$).

Complications

No severe acute reactions were observed. Regarding late reactions, 2 patients developed Grade 2 late skin reactions, 2 patients developed Grade 2 late mucosal reactions, and the other 67 patients had only Grade 0–1 late skin and/or mucosal reactions. Besides a single patient developing Grade 1 late brain reaction, there were no other brain symptoms.

DISCUSSION

After carbon ion radiotherapy with total doses ranging from 52.8 GyE to 64 GyE in 16 fractions over 4 weeks, the overall 5-year local control rate in the 72 patients was 84.1%. The dose per fraction ranged from 3.3 GyE to 4.0 GyE, larger than the dose range traditionally used in photon therapy, and this might have contributed to the improved local control. Harwood *et al.* (26) reported that patients treated with a dose of 4 Gy or more per fraction showed a more favorable complete remission rate than those receiving a dose lower than 4 Gy. Overgaard *et al.* (27) also reported that a high dose per fraction yielded a significantly better response. In the present study, the dose per fraction was ≥3.6 GyE in 94.4% of the patients.

Furthermore, it should be recognized that the increased RBE for malignant melanoma of carbon ions as a high linear energy transfer (LET) radiation might also have favorably affected local control. Blake *et al.* (28) reported that the local recurrence rate after radiotherapy with fast neutrons, also a high LET radiation, was lower than that achieved with X-ray radiotherapy using a large fraction size (16, 17, 29). It is known from cell culture studies that a certain proportion of the damage caused to many cell types by X-rays is sublethal and can be repaired. This could particularly be the case in melanoma cells (30). In this regard, the fact that high LET radiation significantly reduces the potential capacity of damage repair from radiation injury (31) may provide an explanation for the increased effectiveness of high LET beams compared with photon beams in melanoma cells.

Neutron therapy yielding improved local control in selected tumors has not come into wide use because of the high toxicity due to poor dose distributions. Blake *et al.* (28) also reported that, with neutron beams, the incidence of fibrosis and necrosis of the skin was primarily related to the area of the irradiated skin, with such adverse reactions occurring in particular when the area irradiated was >200 cm^2. The use of heavy charged particles like carbon ions exhibiting biologically favorable dose localization can avoid such complications. In the present study, none of the patients developed Grade 3 or higher late skin reactions.

Carbon ion treatment can be completed with relatively small fractions and in a short time. Experiments with neutron beams have demonstrated that increasing their fraction size tended to lower RBE for both the tumor and normal tissues. Relative biological effectiveness of the tumor, however, did not decrease as rapidly as RBE for normal tissues. Similar results from experiments with carbon ion beams have been obtained in our institute (32). These experimental results have substantiated the fact that with high LET radiation the therapeutic ratio increases rather than decreases, even though the fraction dose is increased (33–35), and may explain the good local control without severe normal tissue reactions in our series.

In the present study, the 3-year and 5-year overall survival rates were 46.1% and 27.0%, and the 3-year and 5-year cause-specific survival rates were 47.7% and 39.6%, respectively. Gilligan *et al.* (29) reported an overall survival rate of 17.9% after conventional radiotherapy, and Wada *et al.* (17) reported a 3-year cause-specific survival rate of 33%. Lund *et al.* (12) and Owens *et al.* (7) reported 5-year overall survival rates of 28% and 36%, respectively, in surgical resection studies, in which some of the patients received postoperative radiotherapy (Table 3). Although the patients' stages in the present study did not completely match those in the other studies, the survival rates achieved with carbon ions seemed superior to other radiotherapeutic modalities and were comparable to surgery.

No prognostic factors, including tumor volume, affected local control in the present study. Despite the fact that the tumor volume of more than half of our cases was >100 mL, it was notable that a high local control rate was obtained in our series. In comparison, the reported local control rates of surgical resection were approximately 50% (7–13), whereas in one surgery report 47% of the patients had tumors <5 mm in thickness (8). This points out the advantage of the use of carbon ion beams especially for patients with large tumors in terms of local control.

Table 3. Mucosal malignant melanoma: local recurrence and survival

Authors (reference)/institute/year	Modality	n	Stage (n)*	Local recurrence (%)	Overall survival	
					3 y (%)	5 y (%)
Lund *et al.* (12)/Institute of Laryngology and Otology/1999	Surgery[†]	58[‡]	I/II/III: 58/0/0	—	—	28
Patel *et al.* (8)/MSKCC/2002	Surgery[§]	59[‖]	I/II/III: 47/8/4	50	41	35
Owens *et al.* (7)/MDACC/2003	Surgery[¶]	44	N/A	—	61	36
Wada *et al.* (17)/Northern Japan RTOG/2004	RT	31	I/II/III: 27/4/0	41	33[#]	—
Gilligan *et al.* (29)/Christie Hospital and Holt Radium Institute/1991	RT	28	N/A	39	—	17
NIRS	Carbon	72**	I/II/III: 68/4/0	12.5	46.1	27.0
(Subgroup: tumor volume <100 mL	Carbon	35	I/II/III: 35/0/0	11.4	66.9	62.4)

Abbreviations: MS-KCC = Memorial Sloan-Kettering Cancer Center; MDACC = M. D. Anderson Cancer Center; N/A = not available; RT = radiotherapy; RTOG = Radiation Therapy Oncology Group; NIRS = National Institute of Radiological Sciences.

* Stage I: local disease; Stage II: regional metastasis; Stage III: distant metastasis. (Recurrence cases are included in the NIRS study.)

† 29 cases received surgery alone (S), 29 cases received S plus other modalities.

‡ In 91% of the patients tumor was confined to the nasal cavity.

§ 35 cases received only S, 24 cases received S plus radiotherapy (RT).

‖ In 47% of the patients tumor thickness was less than 5 mm.

¶ 20 cases received only S, 24 cases received S plus RT.

Cause-specific survival.

** In more than 50% of the patients tumor volume was >100 mL.

In the present study multivariate analysis for survival has shown that tumor volume is a statistically significant factor. Thompson *et al.* (36) also reported that the larger the size of the lesion, the more likely the patient was to have a poor clinical outcome. Similarly, Patel *et al.* (8) reported that tumor thickness was one of the predictive factors significantly correlating with the survival rate. Our results are in agreement with these findings.

After carbon ion therapy in the present study, 40 patients developed distant metastasis, with 34 of them (85.0%) remaining without local recurrence. This indicates that, in these patients, systemic micrometastases might have already existed at the time of treatment, and their management would be desired for improving survival. The concurrent use of systemic medications with carbon ion radiotherapy may help to prevent such micrometastases. On the basis of this hypothesis, we have started a new protocol of carbon ion radiotherapy with concomitant use of chemotherapy.

CONCLUSION

Seventy-two patients with mucosal malignant melanoma of the head-and-neck region were treated with carbon ion beams, and an improved local control rate was obtained regardless of tumor volume. Although the survival rate did not exceed that of surgery, in terms of quality of life the high local control rate of the unresectable large tumors was very meaningful by itself. This result in the present study must be considered a positive step in the treatment of mucosal malignant melanoma. Further studies using carbon ion beams will be needed to improve survival.

REFERENCES

1. Takahashi M, Kiyodera M. Malignant tumor. In: Kawamura T, editor. Gendai Hihukagaku Taikei 11. Tokyo: Nakayama shoten; 1982. p. 66–87.
2. Omura K, Takemiya S, Shimada F, *et al.* Malignant melanoma of the head and neck—collective review from six cancer hospitals. *Gan No Rinsho* 1986;32:1511–1518.
3. McLaughlin CC, Wu X-C, Jemal A, *et al.* Incidence of noncutaneous melanomas in the U.S. *Cancer* 2005;103:1000–1007.
4. Chang AE, Karnell LH, Menck HR. The National Cancer Data Base report on cutaneous and noncutaneous melanoma: A summary of 84,836 cases from the past decade. The American College of Surgeons Commission on Cancer and the American Cancer Society. *Cancer* 1998;83:1664–1678.
5. Ohsumi T, Kiyodera M. Statistical study on malignant melanoma in Japan. *Rinsho derma* 1977;19:115–125.
6. Japan Society of Head and Neck Cancer: Cancer Registry Committee. Report of Head and Neck Cancer Registry of Japan: Clinical statistics of registered patients, 2002. *Head Neck Cancer* 2006;32(Suppl.):3.
7. Owens JM, Roberts DB, Myers JN. The role of postoperative adjuvant radiation therapy in the treatment of mucosal melanomas of the head and neck region. *Arch Otolaryngol Head Neck Surg* 2003;129:864–868.
8. Patel SG, Prasad ML, Escrig M, *et al.* Primary mucosal malignant melanoma of the head and neck. *Head Neck* 2002;24:247–257.
9. Manolidis S, Donald P. Malignant mucosal melanoma of the head and neck: Review of the literature and report of 14 patients. *Cancer* 1997;80:1373–1386.
10. Conley J, Hamaker RC. Melanoma of the head and neck. *Arch Otolaryngol* 1974;99:315–319.
11. Lee SP, Shimizu KT, Tran LM, *et al.* Mucosal melanoma of the head and neck: The impact of local control on survival. *Laryngoscope* 1994;104:121–129.

12. Lund VJ, Haward DJ, Harding L, *et al.* Management options and survival in malignant melanoma of the sinonasal mucosa. *Laryngoscope* 1999;109:208–211.
13. Stern SJ, Guillamondegui OM. Mucosal melanoma of the head and neck. *Head Neck* 1991;13:22–27.
14. Moore ES, Martin H. Melanoma of the upper respiratory tract and oral cavity. *Cancer* 1955;8:1167–1176.
15. Rode I. Clinical and radiobiological properties of melanoblastoma. Budapest: Akademiai Kiado; 1968.
16. Trotti A, Peters LJ. Role of radiotherapy in the primary management of mucosal melanoma of the head and neck. *Semin Surg Oncol* 1993;9:246–250.
17. Wada H, Nemoto K, Ogawa Y, *et al.* A multi-institutional retrospective analysis of external radiotherapy for mucosal melanoma of the head and neck in northern Japan. *Int J Radiat Oncol Biol Phys* 2004;59:495–500.
18. Tsujii H, Morita S, Miyamoto T, *et al.* Preliminary results of phase I/II carbon ion therapy at National Institute of Radiological Sciences. *J Brachyther Int* 1997;13:1–8.
19. Tsujii H, Miyamoto T, Mizoe J, *et al.* Experience of carbon ion radiotherapy at NIRS. In: Kogelnik HD, Lukas P, Sedlmayer, editors. Progress in radio-oncology. VII ed. Salzburg: Monduzzi Editore; 2002. p. 393–405.
20. Mizoe J, Tsujii H, Kamada T, *et al.* Dose escalation study of carbon ion radiotherapy for locally advanced head-and-neck cancer. *Int J Radiat Oncol Biol Phys* 2004;60:358–364.
21. Raju MR. Heavy particle radiotherapy. New York: Academic Press; 1980.
22. Prelec K. Ions and ion accelerators for cancer treatment. *FIZIKA B* 1997;6:177–208.
23. Endo M, Koyama-Ito H, Minohara S, *et al.* HIPLAN: A heavy ion treatment planning system at HIMAC. *J Jpn Soc Ther Radiol Oncol* 1996;8:231–238.
24. Kanai T, Endo M, Minohara S, *et al.* Biophysical characteristics of HIMAC clinical irradiation system for heavy-ion radiation therapy. *Int J Radiat Oncol Biol Phys* 1999;44:201–210.
25. Cox JD, Stetz BS, Pajak TF. Toxicity criteria of the Radiation Therapy Oncology Group (RTOG) and the European Organization for Research and Treatment of Cancer (EORTC). *Int J Radiat Oncol Biol Phys* 1995;31:1341–1346.
26. Harwood AR, Cummings BJ. Radiotherapy for mucosal melanomas. *Int J Radiat Oncol Biol Phys* 1982;8:1121–1126.
27. Overgaard J, Overgaard M, Hansen PV, *et al.* Some factors of importance in the radiation treatment of malignant melanoma. *Radiother Oncol* 1986;5:183–192.
28. Blake PR, Catterall M, Errington RD. Treatment of malignant melanoma by fast neutrons. *Br J Surg* 1985;72:517–519.
29. Gilligan D, Slevin NJ. Radical radiotherapy for 28 cases of mucosal melanoma in the nasal cavity and sinuses. *Br J Radiol* 1991;64:1147–1150.
30. Blakely EA. Cell inactivation by heavy charged particles. *Radiat Environ Biophys* 1992;31:181–196.
31. Smith IE, Courtenay VD, Mills J, *et al.* In vitro radiation response of cells from four human tumors propagated in immune-suppressed mice. *Cancer Res* 1978;38:390–392.
32. Koike S, Ando K, Uzawa A, *et al.* Significance of fractionated irradiation for the biological therapeutic gain of carbon ions. *Radiat Prot Dosimetry* 2002;99:405–408.
33. Kraft G. Tumor therapy with heavy charged particles. *Prog Part Nucl Phys* 2000;45:S473–S544.
34. Denekamp J, Waites T, Fowler JF. Predicting realistic RBE values for clinically relevant radiotherapy schedules. *Int J Radiat Biol* 1997;71:681–694.
35. Chen GTY, Castro JR, Quinvey JM. Heavy charged particle radiotherapy. *Ann Rev Biophys Bioeng* 1981;10:499–529.
36. Thompson LD, Wieneke JA, Miettinen M. Sinonasal tract and nasopharyngeal melanoma. *Am J Surg Pathol* 2003;27: 594–611.

ELSEVIER

Int. J. Radiation Oncology Biol. Phys., Vol. 75, No. 4, pp. 1105–1110, 2009

0360-3016/09/$–see front matter

doi:10.1016/j.ijrobp.2008.12.019

CARBON ION RADIOTHERAPY FOR UNRESECTABLE RETROPERITONEAL SARCOMAS

ITSUKO SERIZAWA, M.D.,* KENJI KAGEI, M.D., PH.D.,* TADASHI KAMADA, M.D., PH.D.,* REIKO IMAI, M.D., PH.D.,* SHINJI SUGAHARA, M.D., PH.D.,* TOHRU OKADA, M.D.,* HIROSHI TSUJI, M.D., PH.D.,* HISAO ITO, M.D., PH.D.,† AND HIROHIKO TSUJII, M.D., PH.D.*

*Research Center Hospital for Charged Particle Therapy, National Institute of Radiological Sciences, Chiba, Japan; and †Department of Radiology, Chiba University, Chiba, Japan

Purpose: To evaluate the applicability of carbon ion radiotherapy (CIRT) for unresectable retroperitoneal sarcomas with regard to normal tissue morbidity and local tumor control.
Methods and Materials: From May 1997 to February 2006, 24 patients (17 male and 7 female) with unresectable retroperitoneal sarcoma received CIRT. Age ranged from 16 to 77 years (median, 48.6 years). Of the patients, 16 had primary disease and 8 recurrent disease. Histologic diagnoses were as follows: malignant fibrous histiocytoma in 6, liposarcoma in 3, malignant peripheral nerve sheath tumor in 3, Ewing/primitive neuroectodermal tumor (PNET) in 2, and miscellaneous in 10 patients. The histologic grades were as follows: Grade 3 in 15, Grade 2-3 in 2, Grade 2 in 3, and unknown in 4. Clinical target volumes ranged between 57 cm^3 and 1,194 cm^3 (median 525 cm^3). The delivered carbon ion dose ranged from 52.8 to 73.6 GyE in 16 fixed fractions over 4 weeks.
Results: The median follow-up was 36 months (range, 6–143 months). The overall survival rates at 2 and 5 years were 75% and 50%, respectively. The local control rates at 2 and 5 years were 77% and 69%. No complications of the gastrointestinal tract were encountered. No other toxicity greater than Grade 2 was observed.
Conclusions: Use of CIRT is suggested to be effective and safe for retroperitoneal sarcomas. The results obtained with CIRT were a good overall survival rate and local control, notwithstanding the fact that most patients were not eligible for surgical resection and had high-grade sarcomas. © 2009 Elsevier Inc.

Retroperitoneal, Sarcoma, Carbon ion radiotherapy, Particle radiotherapy, Bone and soft tissue sarcomas.

INTRODUCTION

Surgery is the mainstay of treatment for retroperitoneal soft tissue sarcomas (RPSs). However, complete resection rates are in the range of 40% to 60%. Because of their anatomic location and propensity for spreading extensively, most tumors are advanced at the time of diagnosis, resulting in difficult resection and an inability to achieve negative margins. Many cases of positive margins or recurrence are detected after resection (1–3).

One-third of retroperitoneal tumors are soft tissue sarcomas known to be resistant to radiotherapy (RT), meaning that high-dose photon beams are necessary to achieve local control (LC) (4). In contrast to soft tissue sarcomas (STSs) of the extremity, LC rates greater than 90% are achieved with a combination of wide local excision and RT (5–7).

However, because of the limited radiation tolerance of the retroperitoneal, abdominal, and pelvic organs, adequate radiation doses are difficult to deliver, and toxicity can be significant. Various institutions have advocated preoperative or postoperative external beam RT, intensity-modulated radiation therapy (IMRT), intraoperative electron therapy (IORT), and brachytherapy (BT) for the adjunctive treatment of RPSs, with the goal of improving LC, reducing the likelihood of distant metastasis, and improving overall survival (OS). However, the role of systemic therapy also remains controversial (8, 9).

Between 1997 and 1999, a Phase I/II dose escalation study of CIRT trial for bone and soft tissue sarcomas (BSTSs) was conducted at the National Institute of Radiological Sciences (NIRS) (10, 11). It was concluded that CIRT is an effective local treatment for patients with BSTSs for whom surgical resection is not a viable option, and that CIRT seems to represent a promising alternative to surgery. There was no case of fatal toxicity, and no patient need a colostomy. The morbidity rate of CIRT has so far been quite acceptable. However, in

Reprint requests: Itsuko Serizawa, M.D., Research Center Hospital for Charged Particle Therapy, National Institute of Radiological Sciences, Anagawa 4-9-1, Inage-ku, Chiba 263-8555, Japan. Tel: +81-43-251-2111; Fax: +81-43-206-6506; E-mail: s_itsuko@nirs.go.jp

Conflict of interest: none.
Received Oct 3, 2008, and in revised form Dec 11, 2008. Accepted for publication Dec 11, 2008.

Table 1. Histologic subtypes and grades of 24 patients with retroperitoneal soft tissue sarcomas

Histologic subtype	*n*
MFH	6
Liposarcoma	3
MPNST	3
Ewing/PNET	2
Other	10
Histological grade	
G3 (high grade)	15
G2–3 (high grade)	2
G2 (intermediate grade)	3
G1 (low grade)	0
Unknown	4
Total	24

Abbreviations: MFH = malignant fibrous histiocytoma; MPNST = malignant peripheral nerve sheath tumor.

Study was based on the French Federation of Cancer Centers Sarcoma Group.

A three-tiered grading system was used.

our experience 8 of 64 patients (12.5%) had Grade 3 acute skin reaction and 6 of 60 (10%) had Grade 3 late skin reaction; the critical organs were skin/soft tissues for CIRT. The maximum tolerated dose (MTD) for those with subcutaneous tumor involvement was thought to be 70.4 GyE or less, and the MTD of 73.6 GyE was indicated for patients with no subcutaneous tumor. To confirm these findings, a Phase II clinical trial was conducted using two fixed carbon ion doses (70.4 or 73.6 GyE). There was no difference in LC between the outcomes of the two groups. Therefore, the recommended dose for BSTSs was decided at 70.4 GyE (10).

The purpose of this study was to evaluate the applicability of CIRT for unresectable retroperitoneal sarcomas with regard to normal tissue morbidity and local tumor control.

METHODS AND MATERIALS

From May 1997 to February 2006, 24 patients (17 male and 7 female) with unresectable retroperitoneal sarcomas were treated with CIRT. The median follow-up time of all patients was 36 months (range, 6–143 months) and was retrospectively analyzed. Patients with primary tumors and recurrent tumors were included, but patients with distant metastasis were excluded. Sixteen patients had primary tumors and 8 had recurrent tumors. Twelve of the patients had undergone chemotherapy, all more than 4 weeks prior to the radiotherapy. None of the patients had previously undergone RT. Age ranged from 16 to 77 years (median, 48.4 years). Histologic subtypes were as follows: malignant fibrous histiocytoma (MFH) in 6, liposarcoma in 3, malignant peripheral nerve sheath tumor (MPNST) in 3, Ewing/PNET in 2, and other in 10 patients. The histologic grades were as follows: Grade 3 in 15, Grade 2 to 3 in 2, Grade 2 in 3, and unknown in 4. Most tumors were high-grade sarcomas (≥Grade 2) (Table 1). Of the patients, 21 were diagnosed as inoperable and the other 3 refused operation. Clinical target volumes ranged from 57 cm^3 to 1,194 cm^3 (median, 525 cm^3).

All patients underwent magnetic resonance imaging (MRI), computed tomography (CT), and positron emission tomography (PET). The macroscopic tumor of these images was defined as gross target

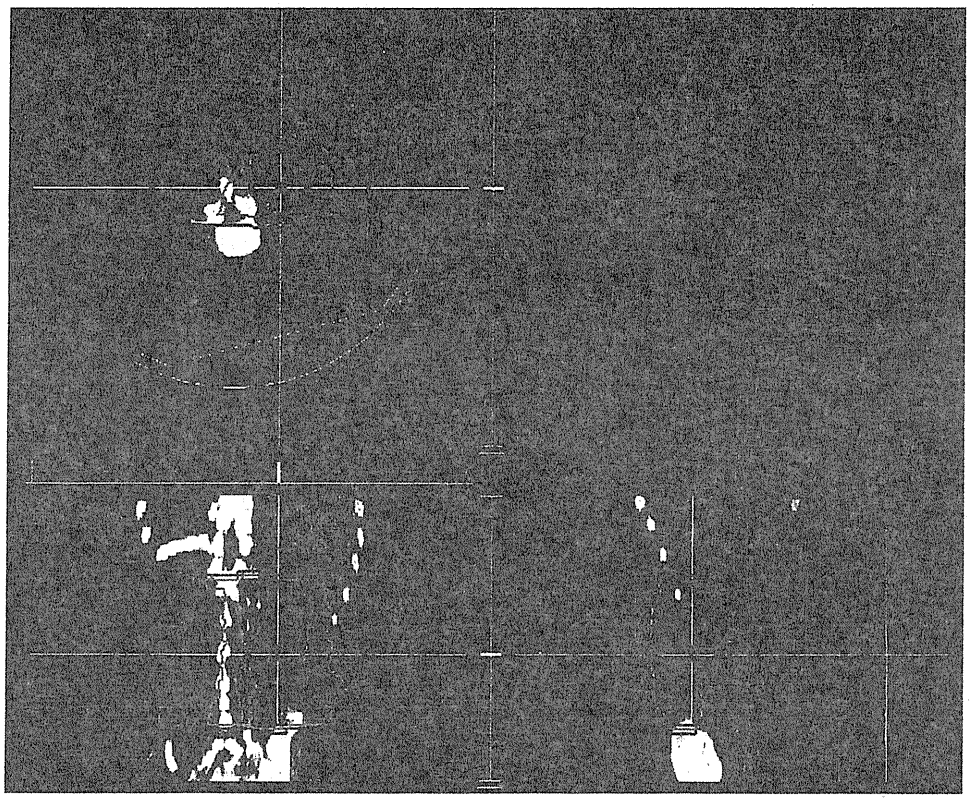

Fig. 1. Dose distribution of carbon ion beam in retroperitoneal sarcoma of malignant fibrous histiocytoma (MFH) (myxoid variant malignant fibrous histiocytoma, myxofibrosarcoma Grade 3) (red line, 90% isodose of the prescribed dose 70.4 GyE/16 fractions/4 weeks with 3 ports). The target volume was 516 cm^3.